

Precision SUSY measurements with ATLAS: SUGRA “Point 4”

Fabiola Gianotti

CERN, PPE Division, 1211 Geneva 23, Switzerland
and
University of Milano, Via Celoria 16, Milano, Italy

This note presents a study of one of the five points of the SuperGRAvity (SUGRA) parameter space studied by ATLAS for the LHCC SUSY Workshop held in October 1996: the so-called “Point 4”. This point is characterised by the following values of the fundamental SUGRA parameters: $m_0 = 800$ GeV, $m_{1/2} = 200$ GeV, $A = 0$, $\tan\beta = 10$, $\text{sign}\mu = +$. For this specific point, the ATLAS discovery potential, as well as the possibility of performing precision measurements of the sparticle masses and thus to determine the fundamental parameters of the theory, are discussed.

1 Introduction

As discussed in [1] the aim of the study presented in this note is twofold. The first goal is to demonstrate that, if Supersymmetry (SUSY) exists and SUGRA is the correct theory and the SUGRA parameters are those of Point 4, a SUSY signal can be observed at the LHC with a reasonable amount of integrated luminosity. Previous studies done for the ATLAS Technical Proposal [2] have shown that this should be relatively easy at the LHC for squark and gluino masses up to 1.5–2 TeV (more or less independently of the model parameters), because the production cross-sections of strongly interacting sparticles (\tilde{q}, \tilde{g}) are large at hadron colliders. The second (and more difficult) goal is, having observed an inclusive SUSY signal, to constrain the parameters of the model (SUGRA or whatever) as much as possible. The most promising way to achieve this second goal is to look for clean (exclusive) signatures which provide constraints on the masses of some sparticles, and therefore on some of the fundamental parameters of the theory. The crucial question is how many SUSY particles can be directly observed at the LHC, and hence how many parameters can be determined and with what precision.

The study presented here has been carried out in the framework of Minimal SuperGRAvity theories with radiative electroweak symmetry breaking (SUGRA [3]). These theories are characterised by a minimal number (five) of independent parameters, thus rendering phenomenological studies practically feasible: a universal scalar mass (m_0), a universal gaugino mass ($m_{1/2}$), a common trilinear interaction term (A), the ratio of the vacuum expectation values of the two Higgs fields ($\tan\beta$) and the sign of the Higgsino mass parameter (μ). R-parity is conserved, therefore the lightest supersymmetric particle (LSP), i.e. the first neutralino χ_1^0 , is stable.

This note is organised as follows. Section 2 describes the model parameters and the SUSY particle spectrum at Point 4. Sections 3 and 4 present the main features of SUSY events at Point 4 and the dominant backgrounds. The semi-inclusive observation of a SUSY signal at Point 4 through the traditional multijet plus missing E_T (\cancel{E}_T) signature and through leptonic signatures are discussed in Section 5 and Section 6 respectively. Sections 7 to 11 describe the reconstruction of exclusive final states and several measurements of sparticle masses: the measurement of the mass difference between the two lightest neutralinos (Section 7), the measurement of the mass of the second chargino (Section 8), the measurement of the mass difference between the gluino and the lighter chargino (Section 9), the measurement of the h -boson mass (Section 10), the measurement of the squark masses (Section 11). The impact of these measurements on the determination of the fundamental parameters of the theory is discussed in Section 12, while Section 13 is devoted to the conclusions.

2 Description of Point 4

This point is characterised by the following values of the parameters in the 5-dimensional SUGRA space:

$$\begin{aligned}
 m_0 &= 800 \text{ GeV} \\
 m_{1/2} &= 200 \text{ GeV} \\
 A &= 0 \\
 \tan\beta &= 10 \\
 \text{sign}\mu &= +
 \end{aligned}$$

from which one can immediately infer that the gluino is relatively light (small gaugino mass $m_{1/2}$), while squarks and sleptons are heavy (large scalar mass m_0).

Once the five fundamental parameters are fixed at the GUT scale, all sparticle masses and couplings at the electroweak scale are obtained by solving the Renormalisation Group Equations (RGE). The Monte Carlo generator used for the study presented here was obtained [1] by interfacing the ISASUSY package of ISAJET 7.22 [4] to SPYTHIA 2.08 [5]. This has allowed to use, on one hand, exact solutions of the RGE equations (which are available in ISAJET but not in SPYTHIA), and, on the other hand, the PYTHIA/JETSET fragmentation package and calculations of the Higgs masses at the two-loop level (which are available in SPYTHIA but not in ISAJET).

The physics spectrum obtained in this way for sparticles at Point 4 is:

$$\begin{aligned}
 m_{\tilde{g}} &= 582 \text{ GeV} \\
 m_{\tilde{q}} &\simeq 915 \text{ GeV} \\
 m_{\tilde{t}_1} &= 594 \text{ GeV} \\
 m_{\tilde{t}_2} &= 805 \text{ GeV} \\
 m_{\tilde{b}_1} &= 774 \text{ GeV} \\
 m_{\tilde{b}_2} &= 903 \text{ GeV} \\
 m_{\tilde{\ell}} &\simeq 800 \text{ GeV} \\
 m_{\chi_{1,2,3,4}^0} &= 80, 148, 290, 315 \text{ GeV} \\
 m_{\chi_{1,2}^\pm} &= 147, 315 \text{ GeV} \\
 m_h &= 111 \text{ GeV (calculated at the two-loop level)} \\
 m_{A,H,H^\pm} &\simeq 860 \text{ GeV}
 \end{aligned}$$

where for the masses of the squarks of the first two generations and of the sleptons an average between the left-handed and the right-handed helicity states has been taken (the mass splitting is about 10 GeV for Point 4).

The main decay modes of these sparticles are listed in Tables 1 and 2. There is good agreement between SPYTHIA (modified as described above) and ISAJET for all decays, except in the stop sector.

From the SUSY masses listed above and from the decay channels presented in Tables 1 and 2 one can deduce several phenomenological consequences and some differences with the other points studied by ATLAS (see Table 3):

- Point 4 is outside the reach of LEP2 and TeVatron, unlike Point 3 where $h, \chi_1^\pm, \chi_1^0, \chi_2^0$ are light enough to be observed at LEP2, and $\chi_1^\pm, \tilde{q}, \tilde{g}$ may be found at the TeVatron. Furthermore, for Point 4 only the h -boson and the charginos/neutralinos are accessible to an e^+e^- Linear Collider of 1 TeV energy or less.
- Since the gluino is relatively light ¹, the total SUSY cross-section is quite large at Point 4 ($\simeq 25$ pb).
- Since the squark mass is larger than the gluino mass, the dominant decay mode of the squarks is $\tilde{q}_{L,R} \rightarrow q\tilde{g}$ (see Table 1), while the direct decay to the LSP $\tilde{q}_R \rightarrow q\chi_1^0$, which dominates if the gluino mass is larger than the squark mass (as for Points 1, 2, 5), has a branching ratio of only a few percent for Point 4. As a consequence, the process $pp \rightarrow \tilde{q}_R\tilde{q}_R$ with both squarks decaying to $q\chi_1^0$, which gives rise to a clean signature consisting of two high- p_T jets accompanied by large \cancel{E}_T and which is clearly observable over the Standard Model (SM) background (mainly Z +jet production with $Z \rightarrow \nu\bar{\nu}$) for instance for Point 1 [6], cannot be extracted from the background for Point 4. Therefore, if a SUSY signal were observed (see Sections 5 and 6) but no excess of pairs of high- p_T jets with large \cancel{E}_T were seen, one would deduce either that the gluino mass is smaller than the squark mass, and therefore exclude part of the parameter space, or that the squark mass is light, so that the two-jet plus \cancel{E}_T signature cannot be observed above the background.

In the case of Point 4, the conclusion would be unambiguous. Since the gluino mass is smaller also than the mass of the lighter stop quark, the decay $\tilde{g} \rightarrow \tilde{t}_1 t$, which has a sizeable branching fraction for Points 1, 2 and 5, is closed. This decay, if open, would give rise to an excess of events containing several b quarks in the final state (four in the case of $\tilde{g}\tilde{g}$ production). Therefore, the absence of an excess of b -tagged jets in a sample of SUSY candidates would indicate that \tilde{t}_1 is (and therefore the other squarks are) heavier than the gluino.

- The mass difference between the two lightest neutralinos is about 70 GeV, i.e. smaller than the h mass and the Z mass. Furthermore squarks and sleptons are heavy at Point 4. As a consequence, the second neutralino can only decay into $Z^*\chi_1^0$. In particular, the channel $\chi_2^0 \rightarrow \chi_1^0 h$, which is the dominant decay mode of the χ_2^0 at Points 1, 2 and 5, and which has been shown to be a very useful handle to select clean SUSY samples, is closed. The absence of a clean peak in the $b\bar{b}$ invariant mass distribution due to h production and decay would allow to exclude the region of the parameter space where the mass difference between the two lightest neutralinos is larger than the h mass.

¹Apart from Point 3, where all sparticles are very light, Point 4 has the lightest gluino mass of all five points studied by ATLAS. This point is also the one with the largest splitting between the squark and the gluino masses.

- Point 4 has the largest slepton masses of all points studied by ATLAS. These masses are outside the reach of LHC, where sleptons are observable only up to masses of ~ 300 GeV [7].
- Since Point 4 has a light gluino and a light χ_1^0 , the event \cancel{E}_T is usually softer than for Points 1, 2 and 5 [8].

3 Signal and background generation

SUSY signal events for Point 4 were generated using SPYTHIA 2.08, modified as described in Section 2, and then passed through the particle-level simulation programme ATLFAST [9].

For inclusive studies, all SUSY processes were switched on at the same time (MSEL = 39 in SPYTHIA). These processes are listed in Table 4 together with their cross-sections. Among the strong processes, which have large cross-sections at the LHC, $\tilde{g}\tilde{g}$ production dominates (since the gluino is light), followed by $\tilde{q}\tilde{q}$ production. On the other hand, since the squarks are heavy in this point, $\tilde{q}\tilde{q}$ production has a much smaller cross-section.

The production of $\chi_1^\pm\chi_2^0$ pairs dominates among the electroweak processes. In some regions of the SUGRA parameter space this channel gives rise to a clean signature in the final state, consisting of three isolated leptons and no hadronic activity (see Section 12). Sleptons are too heavy at Point 4 to be produced with an observable rate ($\sigma < 10^{-5}$ fb).

The SPYTHIA cross-sections are also compared to the ISAJET cross-sections in Table 4. The agreement is in general good, except in a few cases ($\tilde{g}\tilde{q}$ production for instance). In these cases, an average between the two generators has been taken.

The distributions of the transverse momentum of some SUSY particles are shown in Figs. 1 and 2. As expected, the lightest sparticles ($\chi_1^0, \chi_2^0, \chi_1^\pm$) have a softer p_T spectrum, since they are produced at the end of the decay chain.

The following Standard Model processes are the main potential backgrounds to almost all the SUSY channels discussed in this note, since they can result in large missing transverse energy in the final state: $t\bar{t}$ production, if one or both W 's from the top-quarks decay to $\ell\nu$ pairs, W +jet production with $W \rightarrow \ell\nu$, and Z +jet production with $Z \rightarrow \nu\bar{\nu}$. These backgrounds have been generated using PYTHIA and then processed through ATLFAST. A cut of 50–100 GeV on the p_T of the hard-scattering process was applied at the generation level. Table 5 summarises the main features of the background samples which have been used for the analysis described in this note.

4 Event topology at Point 4

Features discriminating SUSY events from Standard Model processes are the large \cancel{E}_T , due to the presence of two χ_1^0 in the final state, and large multiplicity of high- p_T jets and/or leptons, since the produced sparticles are usually heavy and decay through cascade decays.

The expected \cancel{E}_T spectrum, after a pre-selection cut $\cancel{E}_T > 200$ GeV, is shown in Fig. 3 for the SUSY signal and for the dominant SM backgrounds (W/Z+jets, $t\bar{t}$). The multiplicity of jets with $p_T > 15$ GeV reconstructed over the full calorimeter coverage ($|\eta| < 5$) is presented in Fig. 4 after the same pre-selection cut. It can be seen that SUSY events at Point 4 have on average about seven high- p_T jets in the final state, while W+jet and Z+jet events have about three such jets and $t\bar{t}$ events have about five.

Jets were ordered with decreasing p_T . The p_T of the leading jet is shown in Fig. 5 for the SUSY signal sample and the dominant SM backgrounds. Its mean value is about 150 GeV higher for the signal than for the backgrounds. Even more striking is the difference between signal and background for the p_T distribution of the fifth jet in the event (Fig. 6). Requiring five reconstructed jets in the final state would allow to suppress most of the SM background.

The jet flavour is often a useful feature to extract a SUSY signal above the background [6]. Table 6 shows the multiplicity of b -jets in the final state for the SUSY sample and for the background processes. Default values of the b -tagging efficiency and of the contamination from non- b jets have been used: the b -tagging efficiency was assumed to be 60% for b -jets, 10% for c -jets and 1% for gluon and light-quark jets at low luminosity, for jets with $|\eta| < 2.5$. Requiring no b -tagged jets in the final state would allow to reject the $t\bar{t}$ background by a factor of four, whereas asking for one or more b -jets would significantly reduce the W+jet and Z+jet backgrounds.

Leptons are also produced in the cascade decays of SUSY particles, mainly of charginos and neutralinos. Table 7 shows the expected multiplicity of isolated² charged leptons (e, μ) for the SUSY signal and the SM backgrounds (the Z+jet sample was not included here because the Z was forced to decay into $\nu\bar{\nu}$ pairs). Leptons were required to have a transverse momentum $p_T > 10$ GeV and to be within $|\eta| < 2.5$. The expected reconstruction efficiency of 90% per lepton was not included here. It can be seen that the fraction of SUSY events with at least one isolated lepton in the final state is about 30% for Point 4. Requiring no lepton or one lepton does not improve the signal-to-background ratio significantly. The only way to improve this ratio (although at the expense of the signal rate) is to ask for at least two isolated leptons.

The transverse momentum of the leading lepton in the final state is shown in Fig. 7 for the SUSY sample and the SM backgrounds. In contrast to jets, the lepton p_T distribution is similar for the signal and the backgrounds, because in SUSY events leptons are produced at the end of the decay chain and have therefore rather low p_T despite the large mass of the parent sparticle.

5 Semi-inclusive multijet + \cancel{E}_T signature

As suggested by Figs. 3 to 6, the large \cancel{E}_T and the large multiplicity of high- p_T jets in SUSY events can be exploited to observe a semi-inclusive SUSY signal above the SM background at the LHC.

²Throughout this note a lepton is labelled as “isolated” if the transverse energy contained in a cone of size $\Delta R = 0.2$ around the lepton direction is smaller than 10 GeV.

Previous studies [2] had concluded that a minimum \cancel{E}_T cut of 300 GeV was needed to suppress the background coming from QCD multijet production where one or more jets are mismeasured or completely lost in critical regions of the calorimeters (for instance in the barrel/end-cap or end-cap/forward transition regions). The number of SUSY events surviving a cut $\cancel{E}_T > 300$ GeV is expected to be $\sim 38\,000$ after one year of data taking at low luminosity (corresponding to an integrated luminosity of 10^4 pb^{-1}) for the model parameters of Point 4. This signal rate has to be compared with an expected SM background of $\sim 80\,000$ events. Therefore, by only requiring a large \cancel{E}_T in the final state a signal-to-background ratio of ~ 0.5 can be achieved for Point 4. This ratio can be further increased by requiring several high- p_T jets in the final state:

- four jets with $p_T^{1,2,3,4} > 150, 150, 100, 100$ GeV and $|\eta| < 3.2$
- a fifth jet with $p_T^5 > \text{PT5}$ and $|\eta| < 3.2$

The signal rates and the signal-to-background ratios are shown in Table 8 as a function of the cut on the p_T of the fifth jet (PT5). With a cut $p_T^5 > 90$ GeV the signal efficiency is $\sim 5\%$, and about 11 600 SUSY events are expected for an integrated luminosity of 10^4 pb^{-1} , whilst the background is reduced to only 560 events. Therefore the signal should be observed with large significance. The resulting \cancel{E}_T spectrum for signal and background is shown in Fig. 8.

After this selection, the signal consists mainly of $\tilde{q}\tilde{g}$ events (52%), followed by $\tilde{g}\tilde{g}$ (26%) and $\tilde{q}\tilde{q}$ (20%) events, while before any selection the signal is dominated by $\tilde{g}\tilde{g}$ production (40%) followed by $\tilde{q}\tilde{g}$ (29%) and $\tilde{q}\tilde{q}$ (6%) production (see Table 4). Thus, requiring a large number of high- p_T jets and large \cancel{E}_T in the final state increases the squark contribution, as expected since the squark mass is much larger than the gluino mass for Point 4. The background is dominated by $t\bar{t}$ production, which is the SM process with the highest intrinsic jet multiplicity.

In conclusion, as already demonstrated by previous studies, hadronic final states with high jet multiplicity and large \cancel{E}_T should yield a clean semi-inclusive SUSY signal at the LHC. In the case of Point 4 in particular, a significant signal should be observed after a few days of data taking at low luminosity.

6 Semi-inclusive lepton signatures

In addition to hadronic signatures, final states containing charged leptons can also be used to extract semi-inclusive SUSY signals above the SM background at the LHC.

At Point 4 leptons are mainly produced in the following decays of charginos and neutralinos:

Decay	Branching ratio per lepton family
$\chi_2^0 \rightarrow \ell^+ \ell^- \chi_1^0$	3%
$\chi_1^\pm \rightarrow \ell \nu \chi_1^0$	10%
$\chi_2^\pm \rightarrow \chi_1^\pm Z$ with $Z \rightarrow \ell^+ \ell^-$	1%

Previous studies [2, 10] had shown that selecting events containing pairs of same-sign leptons should allow to efficiently reject the SM background ($t\bar{t}$, WW , Z +jets, etc.), where leptons are usually produced with opposite sign. In SUSY processes, on the other hand, several charginos and neutralinos, as well as W and Z -bosons, can be produced in the cascade decays of squarks and gluinos, thus same-sign leptons are often present in the final state.

A search for same-sign lepton pairs has been done for SUSY events at Point 4 using the following cuts:

- Two same-sign isolated leptons with $p_T > 20$ GeV and $|\eta| < 2.5$ were required.
- $\cancel{E}_T > 120$ GeV.
- At least four jets with $p_T^{1,2,3,4} > 120, 70, 70, 70$ GeV respectively and $|\eta| < 3.2$ were required.

For an integrated luminosity of 10^4 pb^{-1} , the expected number of signal events after these cuts is about 1100, while the background, which is dominated by $t\bar{t}$ production with one of the leptons coming from B-hadron decay, amounts to less than 70 events. Thus the signal-to-background ratio would be larger than 15 and also in this case a clean signal would be easy to extract. Furthermore, a measurement of the lepton charge asymmetry in the final state should allow to determine the ratio between the squark and the gluino masses [2]. This possibility, however, has not been investigated in the study presented in this note.

Another interesting signature for Point 4, which not only should allow to observe a semi-inclusive SUSY signal, but also to measure some parameters of the theory, are final states with opposite-sign same-flavour (OS-SF) lepton pairs. To select a clean SUSY sample with this topology, the following cuts were applied:

- Two OS-SF isolated leptons were required.
- The two leptons should satisfy $p_T(\ell_1) > 20$ GeV and $p_T(\ell_2) > 10$ GeV respectively, and both should have $|\eta| < 2.5$.
- $\cancel{E}_T > 200$ GeV.
- At least four jets with $p_T^{1,2,3,4} > 100, 50, 50, 50$ GeV respectively and $|\eta| < 3.2$ were required.

The last two cuts are necessary to reject the SM background (Z+jets, $t\bar{t}$, WW, WZ, ZZ) to a sufficiently low level.

The efficiency of these selection cuts is about 1% for the SUSY signal at Point 4. A reconstruction efficiency of 90% per lepton has been included, but the inefficiency due to charge misidentification has been neglected since it is expected to be small ($< 1\%$ [11]) for the range of transverse momenta of leptons at Point 4 ($\langle p_T \rangle \simeq 60$ GeV, as shown in Fig. 7).

After these cuts about 6500 signal events are expected for an integrated luminosity of $3 \cdot 10^4 \text{ pb}^{-1}$. The dominant remaining background is from $t\bar{t}$ production (550 events), which is thus reduced by a factor $\sim 3.5 \times 10^4$. The other SM backgrounds (Z+jets, WW, WZ and ZZ) are suppressed by the jet multiplicity cut and the \cancel{E}_T cut. The resulting signal-to-background ratio is larger than 10.

In conclusion, leptonic final states offer additional and independent signatures, with respect to hadronic final states, to extract a SUSY signal at Point 4.

7 Measurement of the $\chi_2^0 - \chi_1^0$ mass difference

Figure 9 shows the di-lepton invariant mass distribution for the OS-SF sample (SUSY and $t\bar{t}$ background) selected as described in the previous section. All possible combinations of OS-SF lepton pairs are included in this plot (about 10% of the SUSY events have a third lepton with $p_T > 10$ GeV). Two structures are clearly visible:

- A structure in the region $m_{\ell^+\ell^-} < 75$ GeV, which arises mainly from the decay of the second neutralino (produced for instance in gluino cascade decays) $\chi_2^0 \rightarrow \ell^+\ell^-\chi_1^0$. An end-point in the di-lepton mass distribution for such events is expected at 68 GeV, which is the mass difference between the two lightest neutralinos. This end-point, albeit not very clean, is visible in Fig. 9.
- A second structure is concentrated around the Z mass and indicates the production of Z bosons in SUSY cascade decays. This Z peak is mainly due to the production of the second chargino χ_2^\pm , followed by the decay $\chi_2^\pm \rightarrow Z\chi_1^\pm$. This channel is discussed further in Section 8.

The observation of an invariant mass spectrum such as the one shown in Fig. 9 would clearly indicate the simultaneous production of the lightest (left-hand peak) and the heaviest (right-hand peak) gauginos.

The end-point at $m_{\ell^+\ell^-} \simeq 68$ GeV is obscured in Fig. 9 by the presence of combinatorial background coming from other SUSY events, for instance from $\tilde{g}\tilde{g}$ production with both gluinos decaying to $q\bar{q}'\chi_1^\pm$. However, the contribution from such events, as well as from the residual $t\bar{t}$ background, can be estimated and subtracted by using a sample of events selected with the same cuts as described in Section 6, except that the two leptons are required to have opposite sign and opposite flavour (OS-OF), i.e. $e^+\mu^-$ or $e^-\mu^+$ pairs. About

3300 such events are expected from SUSY production at Point 4 for an integrated luminosity of $3 \cdot 10^4 \text{ pb}^{-1}$. Figure 10 shows the di-lepton invariant mass distribution for the OS-OF SUSY sample, superimposed to the OS-SF SUSY and background distributions already shown in Fig. 9. As expected, the distribution for the OS-OF sample has no distinct structure.

Figure 11 shows the result obtained after subtracting the OS-OF distribution (SUSY plus background) from the OS-SF distribution (SUSY plus background). The end-point of $\chi_2^0 \rightarrow \ell^+ \ell^- \chi_1^0$ decays can now be clearly measured and is well separated from the Z peak.

As already mentioned, the position of the end-point provides an estimate of the mass difference between the two lightest neutralinos. As an example, Fig. 12 shows the di-lepton invariant mass distributions, obtained after subtraction of the OS-OF samples from the OS-SF samples, for two different values of the χ_1^0 mass: $m_{\chi_1^0} = 79 \text{ GeV}$, which is the nominal value for Point 4, and $m_{\chi_1^0} = 87 \text{ GeV}$. The end-point of the distribution moves rapidly, as expected, as a function of the mass difference between the two neutralinos, and therefore a measurement of this end-point will allow a precise determination of this mass difference.

To evaluate the precision of this measurement, several distributions similar to those in Fig. 12 were obtained by varying the χ_1^0 mass by a few GeV around its nominal value, while keeping all other parameters of the model at their default values. A Kolmogorov test [12] was then used to estimate the compatibility between these distributions and the one obtained for the nominal χ_1^0 mass. The resulting precision expected for an integrated luminosity of $3 \cdot 10^4 \text{ pb}^{-1}$ is:

$$m_{\chi_2^0} - m_{\chi_1^0} = 68.13_{-1.0}^{+0.5} \text{ (statistical)} \pm 0.07 \text{ (systematic) GeV}$$

where the first error is the statistical error given by the Kolmogorov test. The systematic error comes from the expected uncertainty on the lepton energy scale at the LHC (0.1%). Experiments at the TeVatron Collider [13], as well as detailed full-simulation studies performed in ATLAS [14], have demonstrated that such a precision is indeed achievable.

For an integrated luminosity of $3 \cdot 10^5 \text{ pb}^{-1}$ the precision of this measurement is expected to improve to

$$m_{\chi_2^0} - m_{\chi_1^0} = 68.13_{-0.32}^{+0.17} \text{ (statistical)} \pm 0.07 \text{ (systematic) GeV}$$

i.e. to about $\pm 0.4\%$, a value still dominated by the statistical error.

8 Measurement of the χ_2^\pm mass

As already mentioned in Section 7, the Z peak in Figs. 9 – 12 is mainly due to the production of the heavier chargino and to its decay $\chi_2^\pm \rightarrow Z\chi_1^\pm$.

The heavier chargino and the two heaviest neutralinos³ are the only sparticles at Point 4 which decay to Z bosons. The branching ratios are 32% for $\chi_2^\pm \rightarrow Z\chi_1^\pm$, 34% for $\chi_3^0 \rightarrow Z\chi_{1,2}^0$ and 5% for $\chi_4^0 \rightarrow Z\chi_{1,2}^0$ (see Table 2).

³Note that χ_2^\pm and χ_4^0 are degenerate in mass in SUGRA models.

These sparticles have large higgsino components in their field content, and therefore their features are sensitive to the parameters of the Higgs sector $\tan\beta$ and μ . Thus a measurement of (for instance) their masses should allow to constrain these parameters.

Charginos and neutralinos are produced in cascade decays of \tilde{q} and \tilde{g} . The branching fractions for these decays listed in Table 1 are not exactly the same in SPYTHIA and ISAJET, therefore an average between the two generators has been taken (where needed) to normalise the expected signal rates. The channel $\chi_2^\pm \rightarrow Z\chi_1^\pm$ dominates over the channels $\chi_{3,4}^0 \rightarrow Z\chi_{1,2}^0$: about 85% of the SUSY events containing a Z in the final state come from the production and decay of the second chargino.

The production cross-section of the second chargino for Point 4, followed by the decay $\chi_2^\pm \rightarrow Z\chi_1^\pm$ and by the Z decay to a lepton pair, has a cross-section of ~ 1 pb (branching ratios included). This rate is large enough to observe a χ_2^\pm signal with a reasonable amount of integrated luminosity.

In order to select a clean sample of SUSY events with a Z in the final state coming from the decay of the second chargino, the cuts discussed in Section 6 have been somewhat tightened:

- Two OS-SF isolated leptons, both with $p_T > 20$ GeV and $|\eta| < 2.5$, were required.
- The invariant mass of the lepton pair was required to be in the range $87 < m_{\ell+\ell^-} < 97$ GeV.
- A third isolated lepton with $p_T > 10$ GeV and $|\eta| < 2.5$ was required.
- $\cancel{E}_T > 100$ GeV.
- At least four reconstructed jets with $p_T > 100, 50, 40, 40$ GeV and $|\eta| < 3.2$ were required.

The last three cuts are needed to reject the potential background coming from SUSY events and SM processes ($t\bar{t}$, WZ, ZZ, Z+jets, Z**b** \bar{b}). After these selection cuts, about 250 signal events, 60 background events from SUSY processes and 4 $t\bar{t}$ events (which are the dominant SM background after all cuts) are expected for an integrated luminosity of $3 \cdot 10^4$ pb^{-1} .

The observed Z production rate in these SUSY events allows to set loose limits on the χ_2^\pm mass:

$$240 < \chi_2^\pm < 400 \text{ GeV}$$

where the lower value corresponds to the sum of the masses of the χ_1^\pm (which will be given by SUGRA once the measurement discussed in the previous section is used to constrain the model) and of the Z. Below this limit, the decay $\chi_2^\pm \rightarrow Z\chi_1^\pm$ is closed and the Z production rate in SUSY events would almost vanish. The upper value corresponds to the χ_2^\pm mass for which the observed Z rate would decrease by a factor of two. These limits are much less stringent than the constraint on the χ_2^\pm mass given by SUGRA (about

± 20 GeV for $3 \cdot 10^4 \text{ pb}^{-1}$, [15]) after all the other measurements discussed in this note are put into the model. However, a direct measurement of the Z rate is important to confirm the predictions of the theory.

Stricter limits on the mass of the second chargino can be obtained by looking at the distribution of the p_T of the Z, which turns out to be sensitive to the χ_2^\pm mass. Figure 13 shows the reconstructed p_T distribution of the Z, obtained for a sample of SUSY events selected as described above and for two values of the χ_2^\pm mass: 315 GeV (nominal value for Point 4) and 360 GeV. The χ_2^\pm mass has been varied in the Monte Carlo by keeping all other parameters of the model unchanged. A shift in the two distributions is clearly visible, which demonstrates the sensitivity of p_T^Z to the chargino mass. The average value of the reconstructed p_T^Z distribution is shown in Fig. 14 as a function of the chargino mass. A difference of 3 GeV in the χ_2^\pm mass would produce a shift of about 1 GeV on the average p_T^Z . Therefore the measurement of the average p_T^Z should determine the mass of the second chargino.

Concerning the precision of this measurement, the statistical error on the mean value of the p_T^Z distribution is expected to be ± 7 GeV (resp. ± 2 GeV) for an integrated luminosity of $3 \cdot 10^4 \text{ pb}^{-1}$ (resp. $3 \cdot 10^5 \text{ pb}^{-1}$), which translates into a statistical uncertainty of ± 21 GeV (resp. ± 7 GeV) on the chargino mass.

Various sources of systematic effects have been considered:

- If the initial state radiation (ISR) is switched off, the average p_T of the Z decreases by ~ 5 GeV. Since, however, α_s is known with a precision of better than 10%, the expected error on the average p_T^Z coming from theoretical uncertainties in the modelling of ISR should not be larger than 0.5 GeV.
- As already mentioned, the uncertainty on the absolute p_T scale is expected to be 0.1% for the leptonic channels. This corresponds to a systematic uncertainty on the average p_T^Z of less than 0.2 GeV.
- The second chargino is mainly produced in gluino cascade decays. Varying the gluino mass by ± 10 GeV has no effect on the p_T^Z distribution. This is because the Z is produced at the end of the cascade decay, thus with little memory of the mass of the original sparticle. Note that, after introducing into SUGRA all other experimental measurements described in this note, the gluino mass at Point 4 would be constrained to about ± 12 GeV for an integrated luminosity of $3 \cdot 10^4 \text{ pb}^{-1}$.
- In the decay of the χ_2^\pm the Z boson is produced together with the lighter chargino, therefore the p_T of the Z is expected to depend on the χ_1^\pm mass. To estimate this dependence, the mass of the χ_1^\pm has been varied by ± 3.5 GeV, which corresponds to the uncertainty given by SUGRA for $3 \cdot 10^4 \text{ pb}^{-1}$ after all other experimental measurements discussed in this note are introduced in the model. The corresponding variation of the average p_T^Z in the final state is ∓ 2.5 GeV. The uncertainty on the χ_1^\pm mass represents therefore the main systematic error of this measurement.

In conclusion, the average p_T of the Z is expected to be determined with an uncertainty of ± 7 (statistical) ± 2.5 (systematic) GeV for an integrated luminosity of $3 \cdot 10^4 \text{ pb}^{-1}$. The resulting measurement of the chargino mass will be:

$$\mathbf{m}_{\chi_2^\pm} = \mathbf{315 \pm 21 \text{ (statistical)} \pm 9 \text{ (systematic) GeV}}$$

for an integrated luminosity of $3 \cdot 10^4 \text{ pb}^{-1}$, and

$$\mathbf{m}_{\chi_2^\pm} = \mathbf{315 \pm 7 \text{ (statistical)} \pm 4 \text{ (systematic) GeV}}$$

for an integrated luminosity of $3 \cdot 10^5 \text{ pb}^{-1}$. Similar results have been obtained by determining the compatibility of distributions similar to those shown in Fig. 13 using a Kolmogorov test.

Finally, since one of the main sources of χ_2^\pm production for Point 4 is the decay $\tilde{g} \rightarrow t b \chi_2^\pm$, the study of the sample of events described in this section may be used to determine the coupling of the gluino to the top quark. This possibility, however, has not been investigated in the study presented here.

9 Measurement of the $\tilde{g} - \chi_2^0$ and $\tilde{g} - \chi_1^\pm$ mass differences

At Point 4 the gluino mass is smaller than the squark mass, therefore the gluino cannot decay to $\tilde{q}q$ pairs as it does at the other four points. Instead, it undergoes three-body decays into a $q\bar{q}$ pair plus a gaugino (see Table 1):

$$\begin{aligned} \tilde{g} &\rightarrow q\bar{q}' \chi_1^\pm && \text{with a branching ratio of } \sim 44\% \\ \tilde{g} &\rightarrow q\bar{q} \chi_2^0 && \text{with a branching ratio of } \sim 27\% \\ \tilde{g} &\rightarrow q\bar{q} \chi_1^0 && \text{with a branching ratio of } \sim 15\% \\ \tilde{g} &\rightarrow q\bar{q}' \chi_2^\pm && \text{with a branching ratio of } \sim 6\% \end{aligned}$$

The distribution of the invariant mass of the two jets produced in the decay channels listed above should be sensitive to the mass difference between the gluino and the relevant gaugino (χ_1^\pm , χ_2^0 , χ_1^0 or χ_2^\pm), in the same way as the dilepton invariant mass distribution for Point 4 is sensitive to the mass difference between the two lightest neutralinos.

Since the branching ratios for the various decay channels are of the same order of magnitude, the final states are quite complicated and it is difficult to isolate a specific decay mode. Several channels have been considered, with the aim of finding a clean signature which would allow to measure the gluino mass:

- $\tilde{g}\chi_1^0$ production with $\tilde{g} \rightarrow q\bar{q}\chi_1^0$. This channel is very clean, and a measurement of the di-jet invariant mass distribution in the final state would determine the mass difference between the gluino and the LSP. Unfortunately the signal is overwhelmed by the Z +jet (with $Z \rightarrow \nu\bar{\nu}$) background and by SUSY combinatorics. Similar arguments apply to $\tilde{g}\tilde{g}$ production with both gluinos decaying to $q\bar{q}\chi_1^0$.

- $\tilde{g}\chi_2^0$ production with $\tilde{g} \rightarrow q\bar{q}\chi_1^0$ and $\chi_2^0 \rightarrow \ell^+\ell^-\chi_1^0$. This channel would allow to measure at the same time the mass difference between the gluino and the LSP and between the two lightest neutralinos. However the cross-section is small ($\sigma \sim 1$ fb, branching ratios included), and there is a large combinatorial background from other SUSY events.
- $\tilde{g}\tilde{q}_L$ production with $\tilde{g} \rightarrow q\bar{q}\chi_1^0$ and $\tilde{q}_L \rightarrow q\chi_1^\pm \rightarrow q\ell\nu\chi_1^0$. This channel is difficult to extract because of the very large W+jet background.
- $\tilde{g}\tilde{g}$ production with $\tilde{g}\tilde{g} \rightarrow q\bar{q}'\chi_1^\pm q\bar{q}\chi_2^0$. This channel has a relatively clean signature for the case where both gauginos decay leptonically, and at the same time an acceptable rate ($\sigma \sim 40$ fb, branching ratios included). It would allow to measure the mass difference between the gluino and the lightest chargino, and between the gluino and the second lightest neutralino. Note that in SUGRA χ_1^\pm and χ_2^0 are degenerate in mass ($\Delta m \leq 1$ GeV).

This last channel thus gives rise to final states containing four high- p_T jets and three leptons (two from χ_2^0 decay and one from χ_1^\pm decay). The potential backgrounds to this topology are $t\bar{t}$, $Zb\bar{b}$, WW , WZ , ZZ production and SUSY combinatorics. The following selection cuts were applied:

- Three isolated leptons with $p_T > 20, 10, 10$ GeV respectively and $|\eta| < 2.5$ were required. Among them, at least one pair of opposite-sign same-flavour leptons was required in addition.
- Four jets with $p_T > 150, 120, 70, 40$ GeV and $|\eta| < 3.2$ were required. The p_T -thresholds were optimised to reject the SM processes listed above.

Figure 15 shows the distribution of the invariant mass of the OS-SF lepton pairs in the final state for the SUSY events selected with these cuts. As in the di-lepton sample described in Section 7 (see Fig. 9), a clean Z peak and an end-point corresponding to the mass difference between the two lightest neutralinos are visible. In order to further reduce the SUSY combinatorics and the SM background, two additional selection cuts were applied:

- In the case of the signal, two of the leptons in the final state come from the decay $\chi_2^0 \rightarrow \ell^+\ell^-\chi_1^0$. Assuming that the end-point in the $m_{\ell+\ell^-}$ -distribution has been observed and measured using the di-lepton sample described in Section 7, it was required that the invariant mass between any pair of OS-SF leptons in the final state be below 72 GeV. This cut rejects all $Z \rightarrow \ell^+\ell^-$ decays, in particular SM background events from $Zb\bar{b}$, WZ , ZZ production.
- Additional jets with $p_T > 40$ GeV and $|\eta| < 5$ were vetoed. This cut reduces the SUSY combinatorics, but rejects also signal events with more than four jets in the final state (coming for instance from ISR). It has an efficiency of $\sim 35\%$ for the signal at low luminosity.

After these selection cuts one expects, for an integrated luminosity of $3 \cdot 10^4 \text{ pb}^{-1}$, about 250 signal events, 30 SUSY events coming from different production processes but containing one \tilde{g} in the final state ($\tilde{q}\tilde{g}$ production, \tilde{q} production with $\tilde{q} \rightarrow \tilde{g}q$) and 18 background events from final states not containing a gluino. Of these latter events, 12 events arise from $t\bar{t}$ production and 6 events from SUSY combinatorics. Therefore, the signal can be cleanly observed above the background.

It should be noticed that since the \cancel{E}_T spectrum is quite soft in this channel (its average value is ~ 160 GeV), no \cancel{E}_T cut has been applied in the selection, which demonstrates that exclusive SUSY channels can be cleanly extracted above the background at the LHC even without requiring large \cancel{E}_T in the final state.

The following step consisted in reconstructing the invariant mass distribution of pairs of jets in the final state. In principle, there are three different ways of combining the four jets in the event two by two. For the signal sample, if all four jets come from the decay of the two gluinos (and not for instance from ISR), one of these combinations is correct while the other two are wrong. In order to reduce the combinatorics, one of the three combinations, i.e. the one which pairs the two highest- p_T jets together and the two lowest p_T jets together, was ignored since in most cases the two highest- p_T jets come from different gluinos. Only two combinations were therefore considered, of which one is correct. In reality, this picture is further complicated by the fact that sometimes the jets which survive the selection cuts are produced by initial state radiation and not by gluino decays.

Figure 16 shows the di-jet invariant mass distribution for the signal events alone (full histogram). As discussed above, there are four entries per event in this plot, out of which two entries are usually correct and two are wrong. The distribution in Fig. 16 clearly shows a falling edge around 440 GeV, which corresponds to the mass difference between the gluino and the χ_1^\pm/χ_2^0 , although a clean end-point is not visible because of the combinatorial background. For comparison, the dashed histogram shows the distribution obtained by plotting only the combination with at least one correct jet pair (i.e. both jets of the pair come from the decay of one of the two gluinos). The falling edge is much more clearly visible in this case.

Figure 17 shows the di-jet invariant mass distribution for the signal and the background ($t\bar{t}$ and SUSY combinatorics). For events containing only one gluino, there are usually one good entry and three wrong entries. For the background with no gluinos all entries are wrong.

Although the end-point in Figs. 16 and 17 is not as clear as in the di-lepton case (see Figs. 11 and 12), the shape of the di-jet invariant mass distribution displays good sensitivity to the mass difference between the gluino and the χ_1^\pm/χ_2^0 . This is demonstrated by Fig. 18, which shows a comparison of the distributions obtained for $m_{\tilde{g}} = 582$ GeV (nominal value for Point 4) and for $m_{\tilde{g}} = 500$ GeV. As in the previous cases, the gluino mass has been varied in SUGRA by keeping all other parameters of the model at their default values. By using a Kolmogorov test to evaluate the compatibility of the distributions obtained for several values of the gluino mass, the following precision on the

mass difference between the gluino and the χ_1^\pm/χ_2^0 has been obtained:

$$\mathbf{m}_{\tilde{g}} - \mathbf{m}_{\chi_1^\pm}/\mathbf{m}_{\chi_2^0} = \mathbf{434}_{-16}^{+5.0} \text{ (statistical)} \pm \mathbf{4.5} \text{ (systematic) GeV}$$

for an integrated luminosity of $3 \cdot 10^4 \text{ pb}^{-1}$, and

$$\mathbf{m}_{\tilde{g}} - \mathbf{m}_{\chi_1^\pm}/\mathbf{m}_{\chi_2^0} = \mathbf{434}_{-5.0}^{+1.6} \text{ (statistical)} \pm \mathbf{4.5} \text{ (systematic) GeV}$$

for an integrated luminosity of $3 \cdot 10^5 \text{ pb}^{-1}$. The systematic error is dominated by the uncertainty of 1% on the jet energy scale.

10 Measurements of the h -boson mass

The masses of the heaviest Higgs bosons (A, H, H^\pm) are close to 900 GeV for Point 4, that is in a region where neither the channels $H, A \rightarrow t\bar{t}$ nor the decays to gaugino pairs ($H, A \rightarrow \chi_1^\pm \chi_2^\pm, \chi_2^0 \chi_2^0$, etc.) are observable above the SM background [16, 17].

The mass of the lightest Higgs boson (h) is about 111 GeV if two-loop corrections are taken into account. Since the channel $\chi_2^0 \rightarrow \chi_1^0 h$ is closed at Point 4, the h is only produced in the decay of the heaviest charginos and neutralinos (see Table 2), thus with much lower rate than at Points 1, 2 and 5 where it is predominantly produced in the decays of the second neutralino. Therefore the production of the h -boson in SUSY cascade decays, followed by the (dominant) decay mode $h \rightarrow b\bar{b}$, suffers, for Point 4, from a large combinatorial background from other SUSY events and from $t\bar{t}$ production. A signal significance of about four may nevertheless be achieved for an integrated luminosity of $3 \cdot 10^4 \text{ pb}^{-1}$.

Besides in cascade decays, the lightest Higgs boson can be also produced in the hard-scattering process (direct production). At Point 4, where both $\tan\beta$ and m_A are relatively large, the h is mainly produced through gluon-gluon fusion and the only experimentally observable decay mode is $h \rightarrow \gamma\gamma$. This channel has a similar rate ($\sigma \simeq 50 \text{ fb}$, branching ratio included) as a Standard Model Higgs boson [16], and should be observed with a statistical significance of about 5.6σ for an integrated luminosity of 10^5 pb^{-1} [18]. With this amount of integrated luminosity, the h -boson mass should be measured with a precision of about 0.3 GeV. This error is dominated by the uncertainties on the absolute energy scale (0.1%) and on the background ($\gamma\gamma$ continuum) subtraction, and should be reduced to 0.2 GeV for the integrated luminosity of $3 \cdot 10^5 \text{ pb}^{-1}$.

11 Measurement of the \tilde{q} masses

The exclusive channels described in the previous sections will allow to observe several gauginos and the lightest Higgs boson. The ensemble of measurements performed with these channels would ultimately constrain the parameters of the model $m_{1/2}$ and $\tan\beta$ to 10% or better (see Section 12). They would also provide a measurement of the universal scalar mass m_0 , although with a poor

accuracy (about ± 200 GeV for an integrated luminosity of $3 \cdot 10^4 \text{ pb}^{-1}$) since the masses of the SUSY particles studied so far depend only weakly on the scalar mass.

In order to improve the sensitivity to m_0 , as well as to observe directly the production of scalar sparticles at Point 4, one should detect at least one of the following classes of sparticles:

- Sleptons: as already mentioned, sleptons are too heavy at Point 4 to be observed directly.
- Squarks of the third generation (\tilde{t} , \tilde{b}): since these sparticles are heavier than the gluino, they are not produced in gluino decays, but only directly in the hard-scattering process. The cross-section for the direct production is quite small (< 300 fb), because the only diagrams which contribute are $q\bar{q}$ and gg annihilation in the s -channel. Furthermore, stop and sbottom decays (see Table 1) suffer from SUSY combinatorial background, due for instance to gluino production followed by the decay $\tilde{g} \rightarrow t\bar{b}\chi_1^\pm$. For these reasons, observation of the squarks of the third generation will be extremely difficult at the LHC if the model parameters are those of Point 4.
- Squarks of the first two generations: the production cross-section for the squarks of the first two generations is much higher (1.6 pb) than for \tilde{t} and \tilde{b} , despite their larger masses. This is because the gluino is light, therefore the t -channel with gluino exchange dominates the production in the case of squarks of the first two generations. As an example, the rate of events containing at least one sbottom in the final state is four times smaller than the rate of events containing at least one squark of the first two generations. The possibility of detecting these squarks has therefore been studied and the results are discussed below.

Several methods have been investigated:

- In most cases (95% for \tilde{q}_R and 66% for \tilde{q}_L) the squarks decay to $\tilde{g}q$. These final states cannot be distinguished from events due to \tilde{g} production, which have a much larger cross-section and which provide a large and irreducible background to such a squark signal.
- Cleaner channels containing only squarks and the LSP in the final state, such as the processes $pp \rightarrow \chi_1^0 \tilde{q}_R$ and $pp \rightarrow \tilde{q}_R \tilde{q}_R$ with $\tilde{q}_R \rightarrow q\chi_1^0$, have also been considered. These channels lead to events containing one or two jets with very high p_T (since the squarks are heavy) and large \cancel{E}_T , and the transverse momentum of the jets is expected to be sensitive to the value of the squark mass [6]. However, the production cross-section before any cuts is only 1 fb for both channels (once the branching ratio for the decay $\tilde{q}_R \rightarrow q\chi_1^0$ is taken into account), therefore the signal would be completely swamped by the the Z +jet background with $Z \rightarrow \nu\bar{\nu}$ and by other SUSY events.

- Since all the experimental measurements described in this note are expected to constrain the \tilde{g} mass to about ± 12 GeV within SUGRA for an integrated luminosity of $3 \cdot 10^4 \text{ pb}^{-1}$, a measurement of the inclusive SUSY cross-section could provide a determination of the squark mass. This cross-section is shown in Table 9 before any cuts and as a function of the average squark mass (where the average is taken over the \tilde{q} flavours and between the left-handed and the right-handed helicity states). As usual, the squark masses have been varied without changing the other parameters of the model. It can be seen that a variation of the average squark mass by ± 200 GeV would change the total cross-section by a factor of 1.5 at most (for a fixed gluino mass). Given the theoretical uncertainties on the absolute cross-section, coming for instance from the limited knowledge of higher-order corrections and of the structure functions, this method would hardly provide a measurement of the squark mass more precise than the range (± 200 GeV) already determined by the other experimental constraints at Point 4. However, such a measurement of the inclusive cross-section could be used to confirm the predictions of the model.
- The total transverse energy observed in the final state should be sensitive to whether particles with a mass close to 1000 GeV (like the squarks) have been produced, rather than particles with mass 600 GeV (like the gluino). This method relies on the large mass splitting between the squarks and the gluino at Point 4.

To investigate further this last and most promising possibility, a semi-inclusive SUSY sample was selected by requiring five jets in the final state with $p_T^{1,2,3,4,5} > 150, 150, 100, 100, 100$ GeV and $\cancel{E}_T > 300$ GeV. These hard cuts, which are similar to those described in Section 5, were chosen to obtain a SUSY sample enriched in squarks and at the same time to suppress the SM background. In fact, about 9 600 SUSY events and only 400 SM background events are expected after these cuts for an integrated luminosity of 10^4 pb^{-1} , and almost 80% of the signal events contain at least one squark in the final state (the sample is dominated by $\tilde{q}\tilde{g}$ production).

The following step consisted in looking for a variable related to the transverse energy in the final state, which could therefore be sensitive to the squark mass. The chosen variable (indicated as E_{Tsum} hereafter) is the scalar sum of the transverse energies of the five highest- p_T jets in the final state. Given the selection cuts described above, E_{Tsum} is larger than 600 GeV by definition. Other variables, which include more jets or \cancel{E}_T , were found to be more sensitive than E_{Tsum} to the value of the gluino mass and to systematic effects (such as initial state radiation), since they include particles with lower p_T .

The distribution of E_{Tsum} is shown in Fig. 19 for the three production sub-processes $\tilde{g}\tilde{g}$, $\tilde{q}\tilde{q}$ and $\tilde{g}\tilde{q}$. As expected, the distribution is harder for events with at least one squark in the final state. The average value of E_{Tsum} is 1323 GeV for $\tilde{g}\tilde{g}$ production, 1459 GeV for $\tilde{g}\tilde{q}$ production and 1517 GeV for $\tilde{q}\tilde{q}$ production. Figure 20 shows the distribution of E_{Tsum} for SUSY events selected as described above (all sub-processes summed together) and for three

different squark masses: $\langle m_{\tilde{q}} \rangle \simeq 715, 915, 1115$ GeV. The average values of the respective distributions are 1356 GeV, 1436 GeV and 1504 GeV. The expected numbers of events for an integrated luminosity of 10^4 pb^{-1} are about 14 200, 9 600 and 7 000 respectively. Figure 20 demonstrates the sensitivity of the E_{Tsum} distribution to the squark mass. More precisely, a variation of 10 GeV of the squark mass would produce a shift of ~ 3.7 GeV in the average value of E_{Tsum} (for a fixed gluino mass).

The precision which can be achieved on the measurement of the squark mass, however, will be limited by systematic effects if the average value of E_{Tsum} is considered. For instance, the expected uncertainty of 1% on the jet energy scale would translate into an uncertainty of about 15 GeV on the average value of the E_{Tsum} distribution, and therefore of about 40 GeV on the average squark mass. On the other hand, the fraction of events with E_{Tsum} larger than a given value is expected to be much less sensitive to such systematic effects.

Figure 21 shows the fraction of selected SUSY events with $E_{Tsum} > 1500$ GeV as a function of the average squark mass. For the nominal average squark mass this fraction is about 36%, and corresponds to about 10 000 observed events for an integrated luminosity of $3 \cdot 10^4 \text{ pb}^{-1}$. From Fig. 21 it can be inferred that an increase of 25 GeV of the average squark mass would produce an increase of this fraction to 37%. The E_{Tsum} threshold of 1500 GeV used here is close to optimal. With a lower threshold, the event fraction would be more sensitive to the value of the gluino mass, whilst with a higher threshold the sensitivity to the knowledge of the exact shape of the high-energy tails would be larger. The fraction of $\tilde{g}\tilde{g}$ events in the SUSY sample with $E_{Tsum} > 1500$ GeV is about 20%.

The total number of SUSY events above the E_{Tsum} threshold does not vary significantly with $m_{\tilde{q}}$: if $m_{\tilde{q}}$ increases, the total SUSY cross-section decreases, but the acceptance of the E_{Tsum} cut increases, so that the total number of events with $E_{Tsum} > 1500$ GeV decreases very slowly for increasing squark masses. Note that a value as high as $m_{\tilde{q}} \sim 1115$ GeV is already inside the region which is theoretically forbidden for reasons of electroweak symmetry breaking [19].

The size of the error bars in Fig. 21 is about $\pm 1\%$ and reflects the following uncertainties:

- The statistical error ($< 0.4\%$ for an integrated luminosity of $3 \cdot 10^4 \text{ pb}^{-1}$).
- A systematic error of about 0.3% coming from the uncertainty in the initial state radiation. When the ISR is completely switched off, the event fraction with $E_{Tsum} > 1500$ GeV decreases by 3%, leading to a systematic uncertainty of 0.3% if α_s is known to 10%.
- A systematic error of 0.8% coming from the expected uncertainty of 1% on the jet energy scale.

Note that the systematic error due to the uncertainty on the exact value of the gluino mass is negligible. This error is about 0.2% when the gluino mass

is varied by ± 40 GeV, i.e. by more than three times the range allowed by SUGRA for an integrated luminosity of $3 \cdot 10^4 \text{ pb}^{-1}$ once all other experimental measurements described in this note are used to constrain the model.

The total systematic error on the event fraction with $E_{Tsum} > 1500$ GeV would therefore amount to 0.9%, which corresponds to an uncertainty of ~ 23 GeV on the average squark mass.

In conclusion, for an integrated luminosity of $3 \cdot 10^4 \text{ pb}^{-1}$ this method would provide the following measurement of the average squark mass (first two generations):

$$\langle m_{\tilde{q}} \rangle = 915 \pm 9 \text{ (statistical)} \pm 23 \text{ (systematic) GeV}$$

Since the total error is dominated by the systematic uncertainty of 1% on the jet energy scale, which is considered as the ultimate goal achievable with the ATLAS calorimetry, the precision of this measurement is not expected to improve significantly at high luminosity.

The complete integral spectrum of E_{Tsum} , which is shown in Fig. 22 for three different values of the average squark mass, has also been studied. A Kolmogorov test applied to these distributions provides a measurement of the squark mass with a precision similar to the result given above.

12 Summary of the measurements and sensitivity to the parameters of the model

The various measurements of SUSY final states for Point 4, discussed in the previous sections, are summarised in Table 10. Also indicated are the accuracies which could be achieved with these measurements for two typical values of the integrated luminosity: $3 \cdot 10^4 \text{ pb}^{-1}$, corresponding to three years of data taking at low luminosity, and $3 \cdot 10^5 \text{ pb}^{-1}$, corresponding to the “ultimate” luminosity which will be collected by the LHC experiments. In most cases, the measurement accuracy would be of a few percent for the initial period at low luminosity, and would improve to an ultimate value of 1% or less.

The particles which can be directly observed if the model parameters are those of Point 4 are the h -boson, the two lightest neutralinos (χ_1^0, χ_2^0), the two charginos, the gluino and the squarks of the first two generations. Sparticles which cannot be easily observed are the sleptons, the heaviest Higgs bosons (A, H, H^\pm), the stops and the sbottoms.

The impact of these measurements on the determination of the fundamental parameters of the theory is discussed in detail in [15], therefore only the main results are summarised here (see Table 11). The universal gaugino mass $m_{1/2}$, which is strongly constrained by two measurements, namely the mass difference between the two lightest neutralinos and the mass difference between the gluino and the second neutralino, would be ultimately extracted with an uncertainty of about 1%. The universal scalar mass m_0 is determined (mainly by the measurement of the squark mass) with an accuracy of better than 5%. The parameter $\tan\beta$ will be constrained to better than 10%, mainly by the

measurements of the h mass and of the χ_2^\pm mass. These two measurements determine also the sign of μ . An integrated luminosity of 10^5 pb^{-1} will be needed to constrain μ as positive, however already with $3 \cdot 10^4 \text{ pb}^{-1}$ more than 65% of the solutions of the fit to the model give a positive μ . Finally, the parameter A is not constrained since it is related to the stop sector [1] where no experimental measurements are possible for Point 4.

The study presented in this note should by no means be considered as a complete analysis of all experimental observations and measurements which can be performed at Point 4, but rather as an example of the ATLAS potential for precision SUSY physics at this point of the parameter space. Other channels may be observed and other measurements may be obtained, which have not been discussed here. For instance, the direct production of $\chi_2^0 \chi_1^\pm$ pairs, followed by the decays $\chi_2^0 \rightarrow \ell^+ \ell^- \chi_1^0$ and $\chi_1^\pm \rightarrow \ell \nu \chi_1^0$, can be detected by looking for final states containing three isolated leptons and no hadronic activity. A signal significance of larger than six should be achieved at Point 4 with an integrated luminosity of $3 \cdot 10^4 \text{ pb}^{-1}$. As another example, it has been shown in [20] that the heaviest neutralino (χ_4^0) can be observed, and the mass difference between χ_4^0 and χ_1^0 can be measured, by looking for final states containing opposite-sign opposite-flavour lepton pairs. In the same reference it is also suggested that the ratio between the event rates in the two populations of Fig. 9 may be used to constrain $\tan\beta$.

These and other measurements will be ultimately combined to cross-check the various observations and to achieve redundant and over-constrained measurements of the parameters of the theory.

Finally, the main aspects of the detector performance which are crucial for the study of Point 4 are: the calorimeter coverage and hermeticity, for a reliable measurement of \cancel{E}_T ; the calibration of the absolute lepton energy scale to 0.1% both in the electromagnetic calorimeter and in the muon system; the calibration of the absolute jet energy scale to 1% in the calorimeters; excellent energy and angular resolution of the electromagnetic calorimeter to detect the h -boson through the decay $h \rightarrow \gamma\gamma$ [14].

13 Conclusions

The work presented in this note, as well as similar studies on the same subject [6, 20, 21, 22], demonstrates that, if SUSY exists, ATLAS will discover it easily and very rapidly up to sparticle masses in the TeV range. It also demonstrates that ATLAS will be able to isolate clean exclusive channels, to perform precise measurements of the masses of several sparticles, and to constrain the fundamental parameters of the theory to within a few percent.

This means that precision SUSY physics will be possible at the LHC, despite the fact that SUSY final states are kinematically badly constrained (due to the presence of the escaping LSP's), that the environment is extremely harsh (pile-up at high luminosity, large QCD backgrounds, etc.), and that all SUSY channels are produced at the same time, thus contributing to the background of each other and producing complicated topologies in the final state. The

main reasons are that the SUSY cross-sections are large, and that the variety of SUSY channels turns out to be an advantage, rather than a disadvantage, because it gives rise to a rich ensemble of topologies, which provide several handles to reject the SM background and allow to observe many sparticles at the same time.

The SUGRA point discussed in this note is not particularly favourable to the LHC. Studies of other points, rather different in terms of particle spectrum, decay modes and event topology, have reached similar conclusions [6, 20, 21, 22]. These results open new scenarios for SUSY physics at the LHC, shifting the emphasis from the discovery to the precision measurements, and demonstrate once more the potential of the LHC for physics beyond the Standard Model.

Acknowledgements

I am grateful to the members of the ATLAS SUSY Working Group for many useful and stimulating discussions. In particular I would like to thank Daniel Froidevaux, Ian Hinchliffe, Frank Paige, Luc Poggioli, Giacomo Pole-sello, Elzbieta Richter-Was and Marjorie Shapiro. I am also grateful to Steve Mrenna for his help with the SPYTHIA Monte Carlo and to Igor Gavrilenko for his help with the Kolmogorov test.

References

- [1] ATLAS Internal Note PHYS-No-107.
- [2] ATLAS Collaboration, Technical Proposal, CERN/LHCC/94-43.
- [3] M. Drees and S. Martin, in “Electroweak Symmetry Breaking and New Physics at the TeV Scale”, editors T. Barklow, S. Dawson, H. Howard and J. Siegrist, World Scientific Singapore.
- [4] F. Paige and S. Protopopescu, in Supercollider Physics, p. 41, editor D. Soper, World Scientific Singapore, 1986.
- [5] S. Mrenna, SPYTHIA 2.08, ANL-HEP-PR-96-63, Sept. 1996.
- [6] E. Richter-Was, D. Froidevaux and J. Soderqvist, ATLAS Internal Note PHYS-No-108.
- [7] L. Poggioli, transparencies shown at the ATLAS SUSY WG meeting, 24/10/96.
- [8] F. Paige, ATLAS Internal Note PHYS-No-085.
- [9] E. Richter-Was, D. Froidevaux and L. Poggioli, ATLAS Internal Note PHYS-No-079.
- [10] H. Baer et al., “Signals from Minimal Supergravity at the CERN Large Hadron Collider II: Multilepton Channels”, FSU-HEP-951215.

- [11] ATLAS Collaboration, Inner Detector Technical Design Report Vol. 1, ATLAS TDR 4, CERN/LHCC/97-16.
- [12] See for instance Eadie et al., *Statistical Methods in Experimental Physics*, North-Holland, 1971, p. 269.
- [13] F. Abe et al., *Phys. Rev. Lett.* 75, 11 (1995).
- [14] ATLAS Collaboration, Calorimeter Performance Technical Design Report, ATLAS TDR 1, CERN/LHCC/96-40.
- [15] ATLAS Internal Note PHYS-No-112.
- [16] E. Richter-Was et al., ATLAS Internal Note PHYS-No-074.
- [17] D. Froidevaux, talk given at the LHCC SUSY Workshop, 30/10/96, <http://atlasinfo.cern.ch/Atlas/GROUPS/PHYSICS/SUSY/susy.html>.
- [18] E. Richter-Was et al., ATLAS Internal Note PHYS-No-048.
- [19] F. Paige, talk given at the LHCC SUSY Workshop, 30/10/96, <http://atlasinfo.cern.ch/Atlas/GROUPS/PHYSICS/SUSY/susy.html>.
- [20] I. Hinchliffe et al., “Precision SUSY measurements at LHC”, LBNL-39412.
- [21] ATLAS Internal Note PHYS-No-109.
- [22] G. Polesello et al., ATLAS Internal Note PHYS-No-111.

Table 1: *Main decay modes and branching ratios (BR) of the gluino and sfermions at Point 4, as given by SPYTHIA 2.08 and ISAJET 7.22.*

Particle	Decay channel	BR (%) SPYTHIA 2.08	BR (%) ISAJET 7.22
$\tilde{g} \rightarrow$	$q\bar{q}'\chi_1^\pm$	47 (13 for $t\bar{b}$)	40 (10 for $t\bar{b}$)
	$q\bar{q}\chi_2^0$	27	28
	$q\bar{q}\chi_1^0$	14 (2.4 for $t\bar{t}$)	15 (3.2 for $t\bar{t}$)
	$q\bar{q}'\chi_2^\pm$	9 (7 for $t\bar{b}$)	4 (2.6 for $t\bar{b}$)
	$q\bar{q}\chi_4^0$	1.6 (0.7 for $b\bar{b}$)	2 (1 for $b\bar{b}$)
	$g\chi_{3,4}^0$	0	6
$\tilde{q}_L \rightarrow$	$q\tilde{g}$	65	70
	$q'\chi_1^\pm$	17	15
	$q'\chi_2^\pm$	5	4
	$q\chi_2^0$	9	8
$\tilde{q}_R \rightarrow$	$q\tilde{g}$	95	95
	$q\chi_1^0$	5	5
$\tilde{b}_1 \rightarrow$	$b\tilde{g}$	33	38
	$t\chi_2^-$	35	31
	$t\chi_1^-$	17	17
	$W\tilde{t}_1$	3.9	2.8
	$b\chi_2^0$	8	7.7
$\tilde{b}_2 \rightarrow$	$b\tilde{g}$	97	98
$\tilde{t}_1 \rightarrow$	$b\chi_2^+$	49	35
	$b\chi_1^+$	1.4	17
	$t\chi_4^0$	23	9
	$t\chi_3^0$	16	25
	$t\chi_2^0$	1.5	6
	$t\chi_1^0$	8	8
$\tilde{t}_2 \rightarrow$	$t\tilde{g}$	28	34
	$b\chi_1^+$	23	12
	$b\chi_2^+$	~ 0	7
	$t\chi_2^0$	11	6.5
	$t\chi_3^0$	19	15
	$t\chi_4^0$	12	20
$\tilde{\ell}_L^\pm \rightarrow$	$\nu\chi_1^\pm$	46	47
	$\nu\chi_2^\pm$	13	12
	$\nu\chi_1^\pm$	7	7
	$\ell\chi_2^0$	31	31
$\tilde{\ell}_R^\pm \rightarrow$	$\ell\chi_1^0$	95	95
$\tilde{\nu} \rightarrow$	$\ell^\pm\chi_1^\pm$	56	56
	$\ell^\pm\chi_2^\pm$	5	4
	$\nu\chi_1^0$	12	12
	$\nu\chi_2^0$	20	21

Table 2: Main decay modes and branching ratios (BR) of the gauginos at Point 4, as given by SPYTHIA 2.08 and ISAJET 7.22.

Particle	Decay channel	BR (%) SPYTHIA 2.08	BR (%) ISAJET 7.22
$\chi_2^0 \rightarrow$	$q\bar{q}\chi_1^0$	72	72
	$\nu\bar{\nu}\chi_1^0$	18	18
	$\ell\bar{\ell}\chi_1^0$	9	9
$\chi_3^0 \rightarrow$	$W\chi_1^\pm$	66	64
	$h\chi_1^0, h\chi_2^0$	3	3
	$Z\chi_1^0$	16	15
	$Z\chi_2^0$	18	19
$\chi_4^0 \rightarrow$	$W\chi_1^\pm$	74	74
	$h\chi_1^0$	8	8
	$h\chi_2^0$	12	12
	$Z\chi_1^0$	3	3
	$Z\chi_2^0$	2	2
$\chi_1^\pm \rightarrow$	$q\bar{q}'\chi_1^0$	66	66
	$\ell\nu\chi_1^0$	33	33
$\chi_2^\pm \rightarrow$	$W\chi_2^0$	44	43
	$h\chi_1^\pm$	16	17
	$Z\chi_1^\pm$	32	32
	$W\chi_1^0$	7	7

Table 3: Some SUGRA parameters and particle masses (in GeV) for the five points studied by ATLAS.

Point	m_0	$m_{1/2}$	$m_{\tilde{g}}$	$m_{\tilde{q}_R}$	$m_{\tilde{t}_1}$	$m_{\tilde{\ell}_R}$	$m_{\chi_1^0}$	$m_{\chi_1^\pm}$	m_h	m_{A,H,H^\pm}
1	400	400	1004	925	645	430	168	325	95	1045
2	400	400	1008	933	710	431	168	321	115	740
3	200	100	298	313	260	207	45	96	68	375
4	800	200	582	910	594	805	80	147	111	860
5	100	300	767	664	440	157	122	232	93	700

Table 4: Production cross-sections for the main SUSY processes at Point 4, as given by SPYTHIA 2.08 and ISAJET 7.22.

Process	σ (pb) SPYTHIA 2.08	σ (pb) ISAJET 7.22
$\tilde{g}\tilde{g}$	10.5	11.2
$\tilde{g}\tilde{q}$	5.8	8.8
$\tilde{q}\tilde{q}$	1.6	1.6
$\tilde{t}\tilde{t}$	0.28	0.26
$\tilde{g}\chi^0, \tilde{g}\chi^\pm$	0.25	0.28
$\tilde{q}\chi^0, \tilde{q}\chi^\pm$	0.2	0.2
$\chi_1^\pm\chi_2^\pm$	2.0	1.1
$\chi^\pm\chi^0$	3.2	3.4
$\chi_1^\pm\chi_2^0$	2.8	3.1
$\chi^0\chi^0$	0.1	0.2
Total	24.1	27.1

Table 5: For the dominant background processes considered in this note, the cut applied at event generation to the hard-scattering process (p_T^{gen}), the production cross-sections and the total Monte Carlo statistics generated.

Process	p_T^{gen} (GeV)	σ (pb)	Number of generated events
W+jets, $W \rightarrow \ell\nu$	100	1633	$8 \cdot 10^5$
Z+jets, $Z \rightarrow \nu\bar{\nu}$	50	640	$8 \cdot 10^5$
$t\bar{t}$	100	327	$6.75 \cdot 10^5$

Table 6: Average multiplicity of b-jets reconstructed with $p_T > 15$ GeV and $|\eta| < 2.5$ for the SUSY signal and the dominant SM backgrounds, after a pre-selection $\cancel{E}_T > 200$ GeV. The default values for the b-tagging efficiency and the contamination from non-b jets have been assumed (see text).

Process	Event fraction			
	$N_b=0$	$N_b=1$	$N_b=2$	$N_b > 2$
SUSY	47%	29%	18%	6%
W+jets	93%	6%	0.7%	0.4%
Z+jets	92%	7.5%	0.9%	0.3%
$t\bar{t}$	27%	48%	23%	2%

Table 7: Average multiplicity of isolated leptons (e, μ) reconstructed with $p_T > 10$ GeV and $|\eta| < 2.5$ for the SUSY signal and the dominant SM backgrounds, after a pre-selection $\cancel{E}_T > 200$ GeV.

Process	Event fraction			
	$N_{lep}=0$	$N_{lep}=1$	$N_{lep}=2$	$N_{lep} > 2$
SUSY	67%	26%	6%	0.9%
W+jets	58%	42%	0.1%	0
$t\bar{t}$	49%	46%	5.3%	0

Table 8: *Expected signal rate (S) for an integrated luminosity of 10^4 pb^{-1} and expected signal-to-background ratio (S/B) for Point 4 as a function of the cut on the p_T of the fifth jet in the final state ($PT5$). Events have been pre-selected requiring $\cancel{E}_T > 300 \text{ GeV}$ and at least four high- p_T reconstructed jets (see text).*

PT5 (GeV)	S	S/B
0	19300	9
50	17700	12
70	15200	14
90	11600	21
100	9600	23

Table 9: *Inclusive SUSY production cross-section for Point 4 as a function of the average squark mass. The third column gives the ratio between the cross-section for a given squark mass and the cross-section for the nominal squark mass ($\langle m_{\tilde{q}} \rangle = 915 \text{ GeV}$).*

$\langle m_{\tilde{q}} \rangle$ (GeV)	σ (pb)	$\sigma/\sigma_{\text{nominal}}$
715	40.5	1.5
815	31.0	1.2
915 (nominal)	26.2	1.0
1015	23.3	0.9
1115	21.2	0.8

Table 10: *Possible measurements at Point 4 and expected experimental accuracies for integrated luminosities of $3 \cdot 10^4 \text{ pb}^{-1}$ and $3 \cdot 10^5 \text{ pb}^{-1}$.*

Measurement	Expected accuracy (GeV)	
	$3 \cdot 10^4 \text{ pb}^{-1}$	$3 \cdot 10^5 \text{ pb}^{-1}$
$m_h = 111 \text{ GeV}$		$+0.2$ -0.2
$m_{\chi_2^0} - m_{\chi_1^0} = 68 \text{ GeV}$	$+0.5$ -1.0	$+0.18$ -0.33
$m_{\chi_2^\pm} = 315 \text{ GeV}$	$+23$ -23	$+8$ -8
$m_{\tilde{g}} - m_{\chi_2^0}/m_{\chi_1^\pm} = 434 \text{ GeV}$	$+6.7$ -17	$+4.8$ -6.7
$\langle m_{\tilde{q}} \rangle = 915 \text{ GeV}$	$+25$ -25	$+23$ -23

Table 11: *Expected accuracy for the extraction of the fundamental parameters of the SUGRA model at Point 4 for integrated luminosities of $3 \cdot 10^4 pb^{-1}$ and $3 \cdot 10^5 pb^{-1}$.*

Parameter	Expected accuracy	
	$3 \cdot 10^4 pb^{-1}$	$3 \cdot 10^5 pb^{-1}$
$m_0 = 800 \text{ GeV}$	$\pm 50 \text{ GeV}$	$\pm 35 \text{ GeV}$
$m_{1/2} = 200 \text{ GeV}$	$\pm 4 \text{ GeV}$	$\pm 1.5 \text{ GeV}$
$\tan\beta = 10$	± 2	± 0.6
$\text{sign}\mu = +$	unconstrained	constrained
$A = 0$	unconstrained	unconstrained

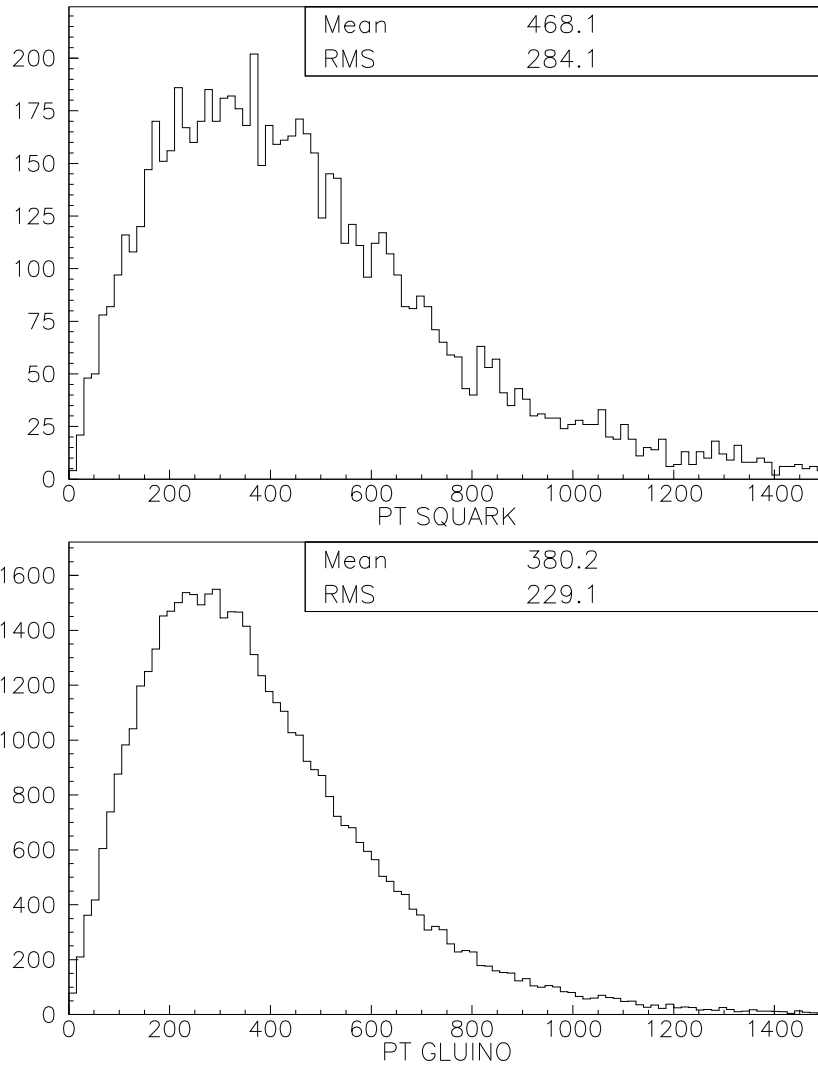


Figure 1: Distributions of the transverse momentum (in GeV) of \tilde{q} (top) and \tilde{g} (bottom) for Point 4.

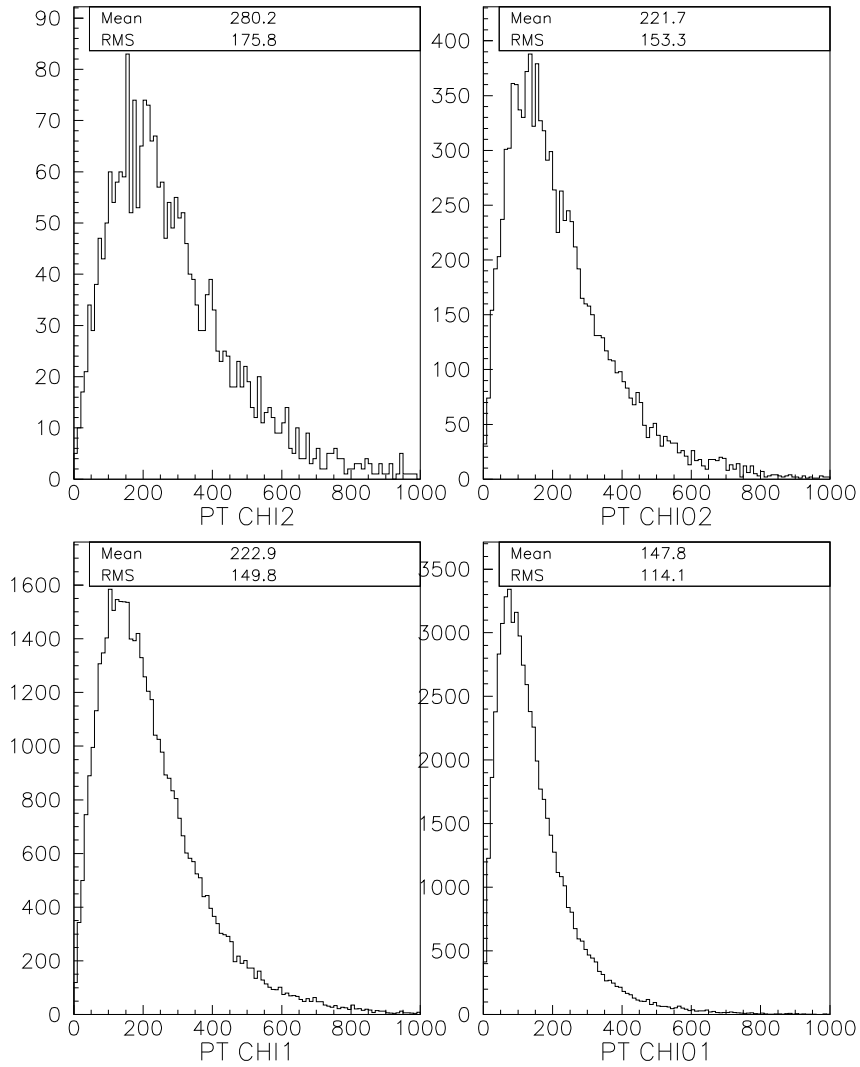


Figure 2: Distributions of the transverse momentum (in GeV) of χ_2^\pm (top left), χ_2^0 (top right), χ_1^\pm (bottom left) and χ_1^0 (bottom right) for Point 4.

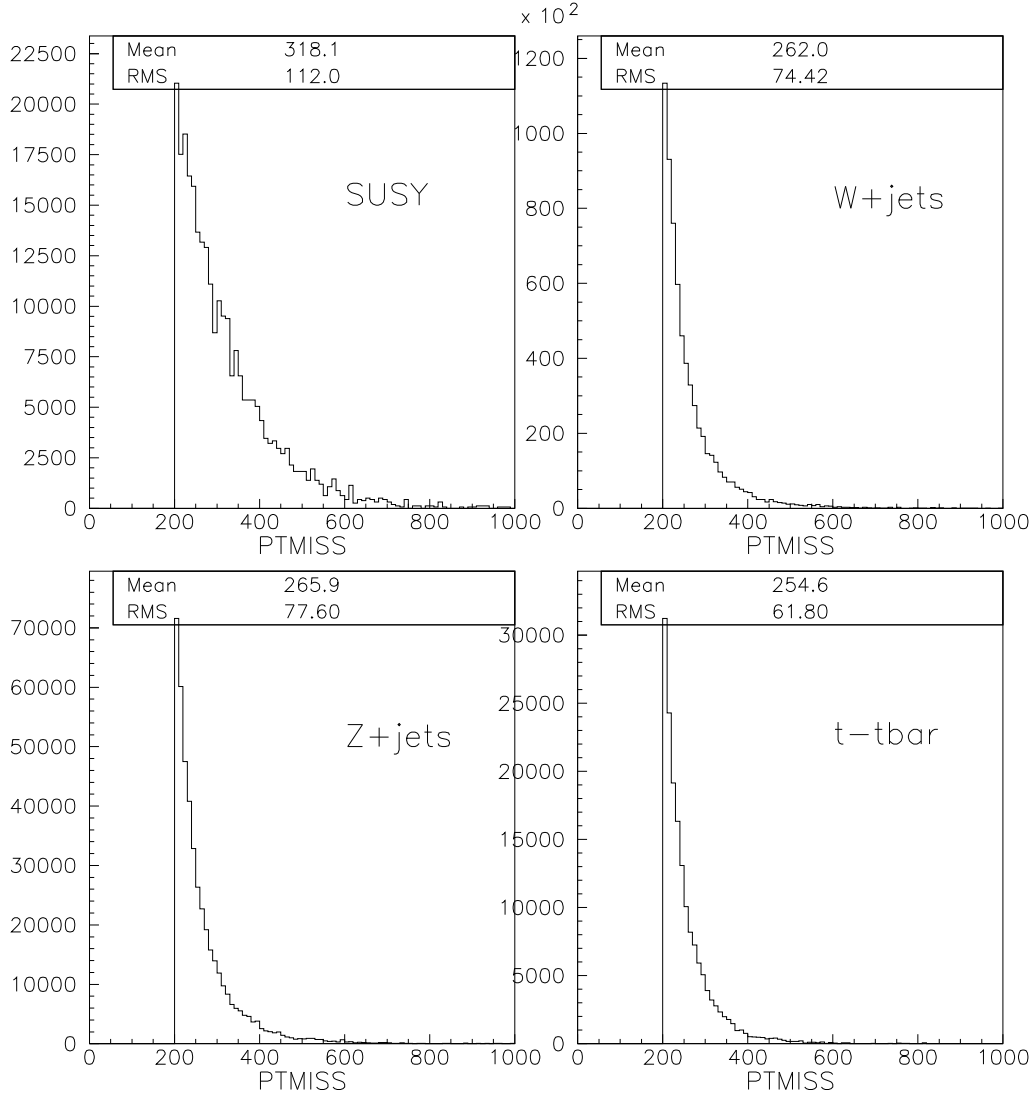


Figure 3: *Distribution of the event missing transverse energy (in GeV) for the SUSY signal and the dominant background processes, after a pre-selection $\cancel{E}_T > 200$ GeV.*

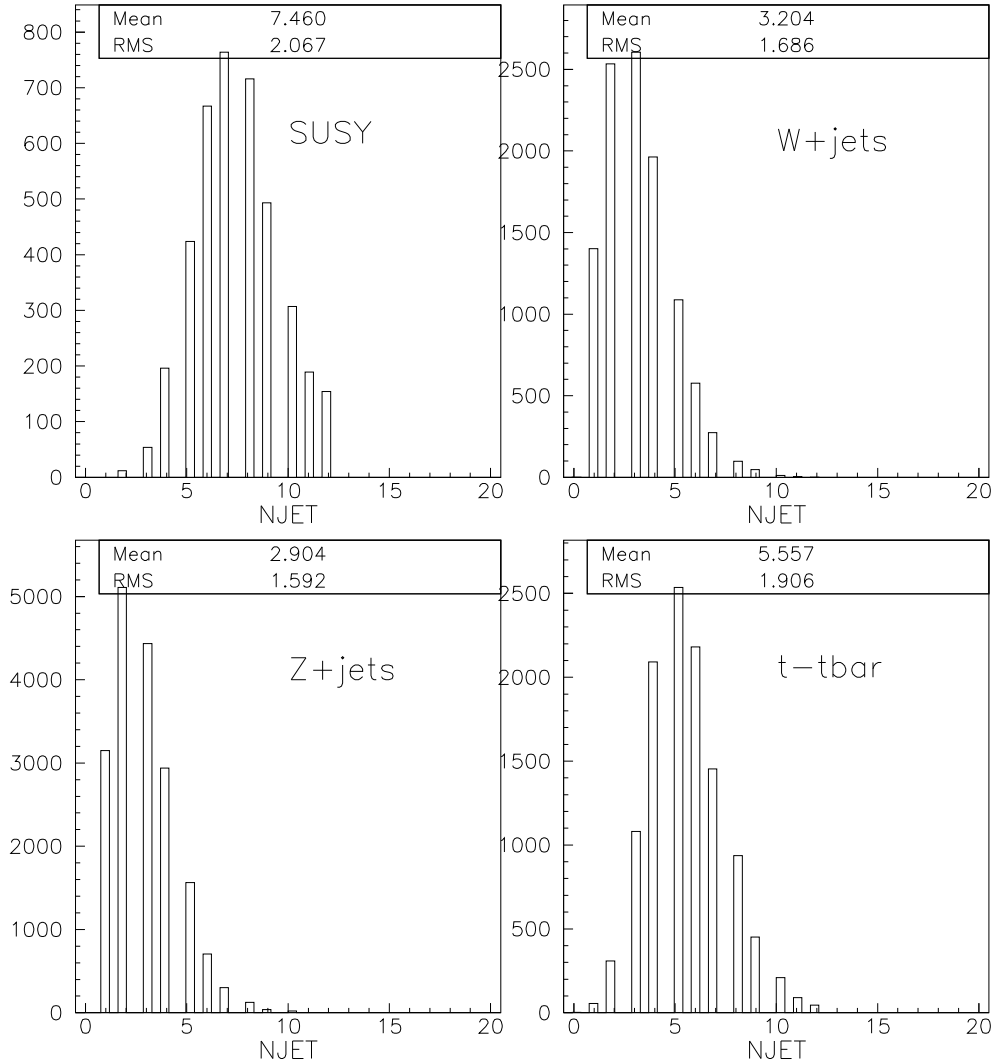


Figure 4: *Multiplicity of reconstructed jets with $p_T > 15$ GeV for the SUSY signal and the dominant background processes, after a pre-selection $\cancel{E}_T > 200$ GeV.*

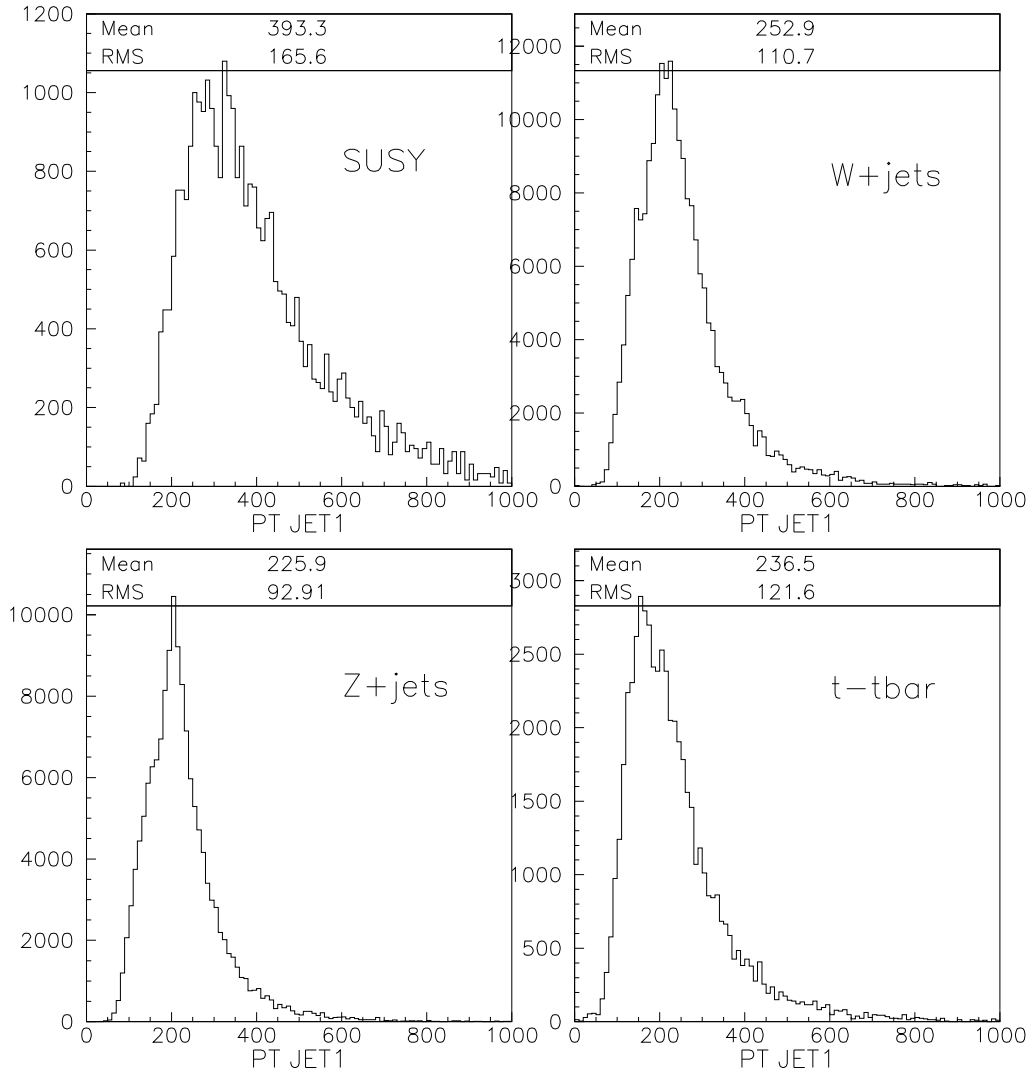


Figure 5: Distribution of the transverse momentum (in GeV) of the leading jet for the SUSY signal and the dominant background processes, after a pre-selection $\cancel{E}_T > 200$ GeV.

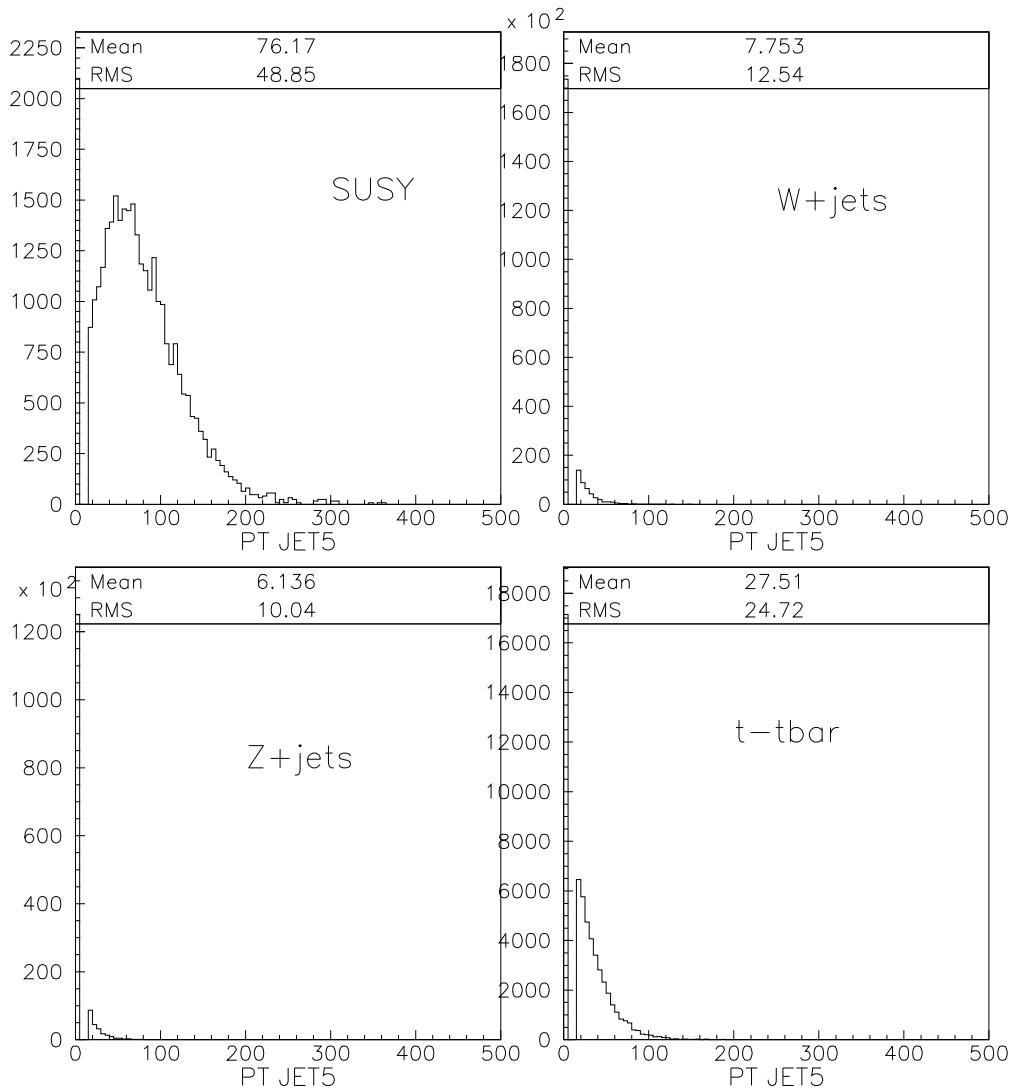


Figure 6: *Distribution of the transverse momentum (in GeV) of the fifth jet for the SUSY signal and the dominant background processes, after a pre-selection $\cancel{E}_T > 200$ GeV.*

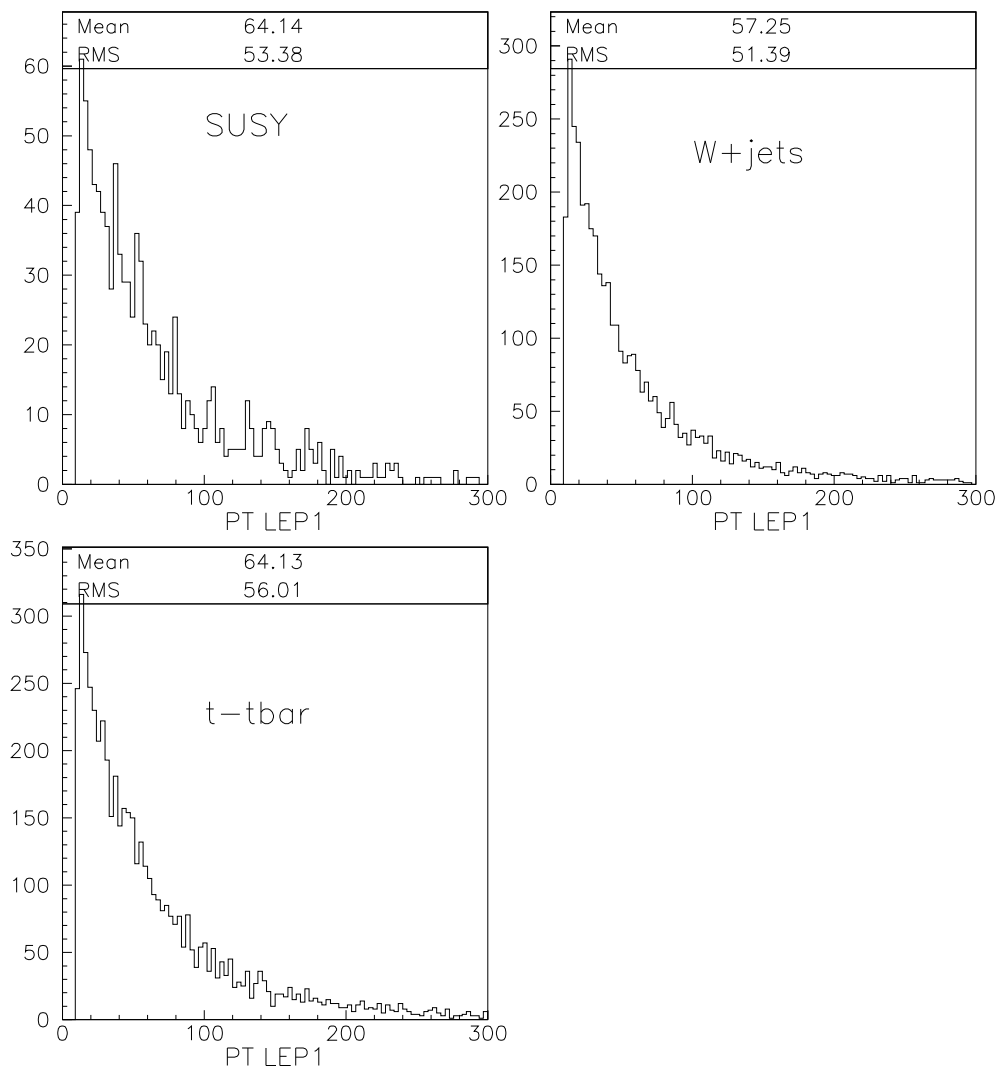


Figure 7: Distribution of the transverse momentum (in GeV) of the leading charged lepton for the SUSY signal and the dominant background processes, after a pre-selection $\cancel{E}_T > 200$ GeV.

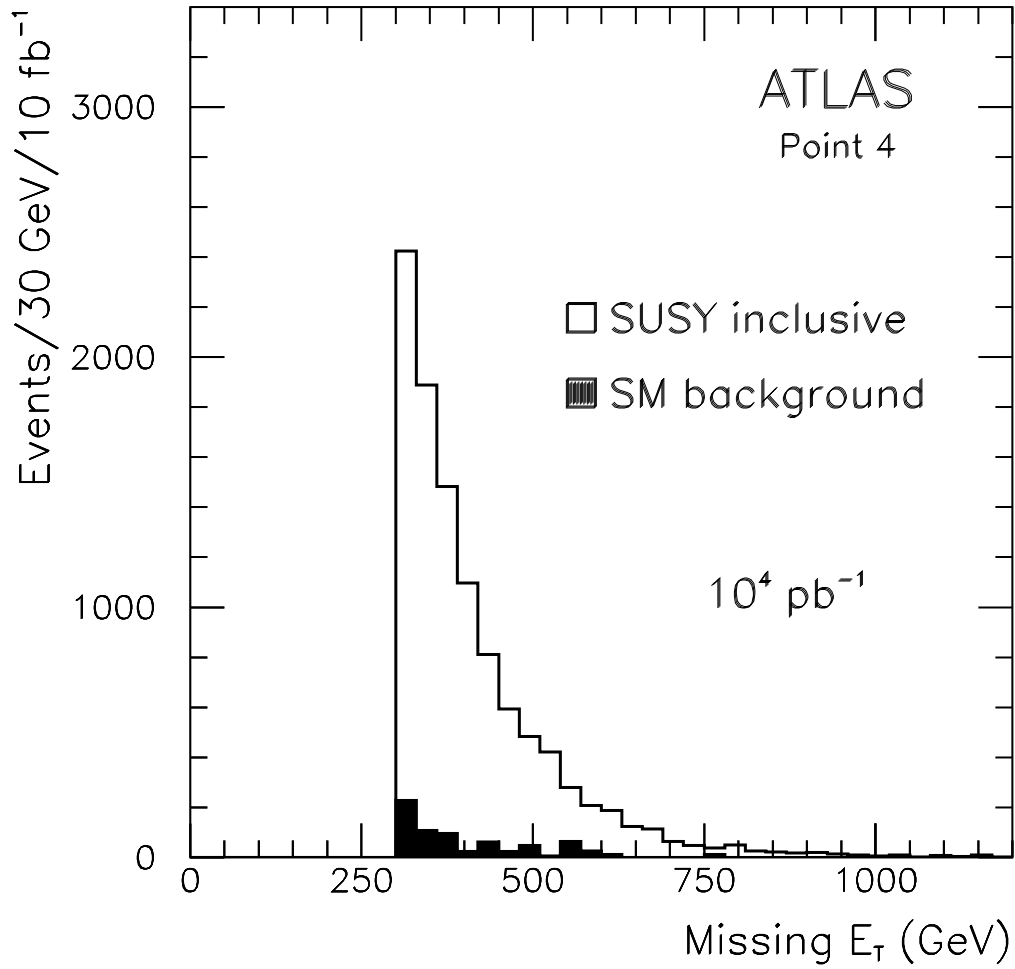


Figure 8: *Expected \cancel{E}_T spectrum for a semi-inclusive SUSY signal at Point 4 (white histogram) and the SM background (black histogram) in ATLAS after one year of data taking at low luminosity. Events with $\cancel{E}_T > 300$ GeV and five high- p_T reconstructed jets are shown (see text).*

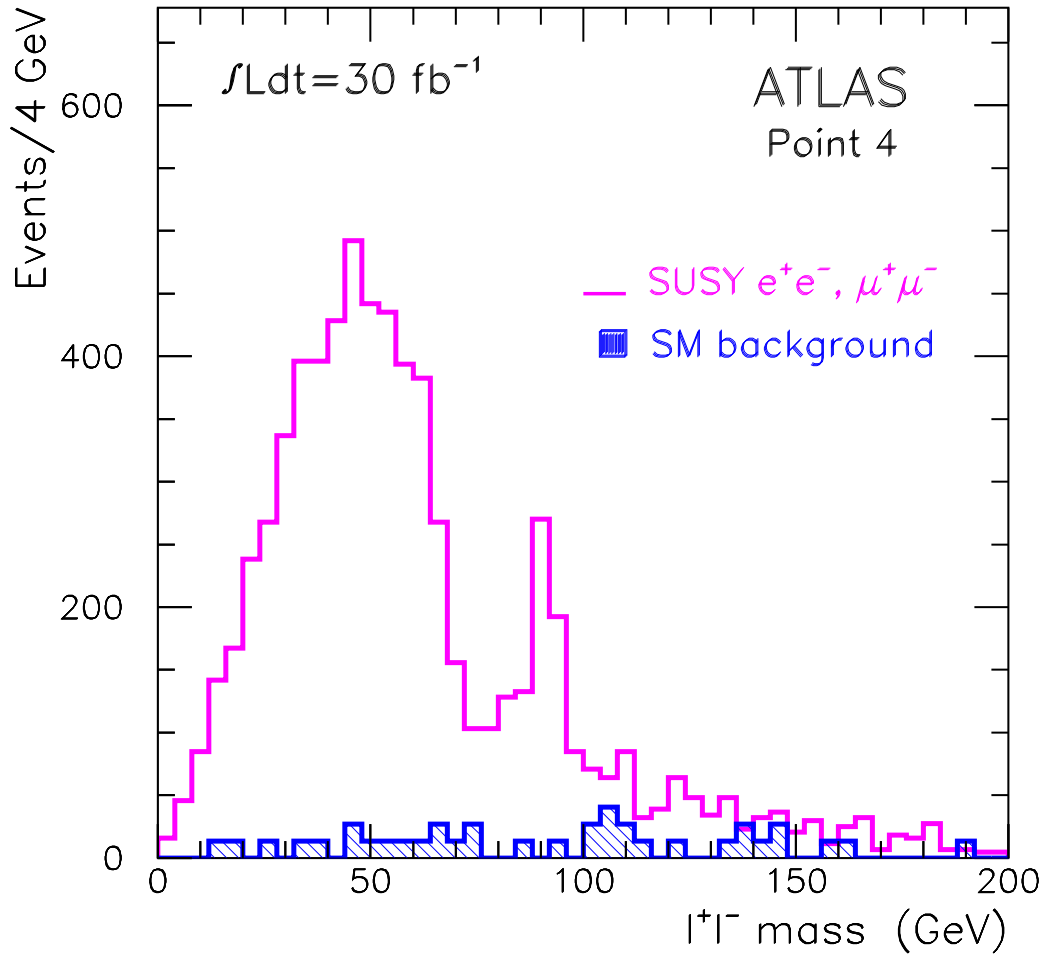


Figure 9: *Expected di-lepton invariant mass distributions for SUSY events containing opposite-sign same-flavour lepton pairs at Point 4 (full histogram) and for the $t\bar{t}$ background (dashed histogram), for an integrated luminosity of $3 \cdot 10^4 \text{ pb}^{-1}$.*

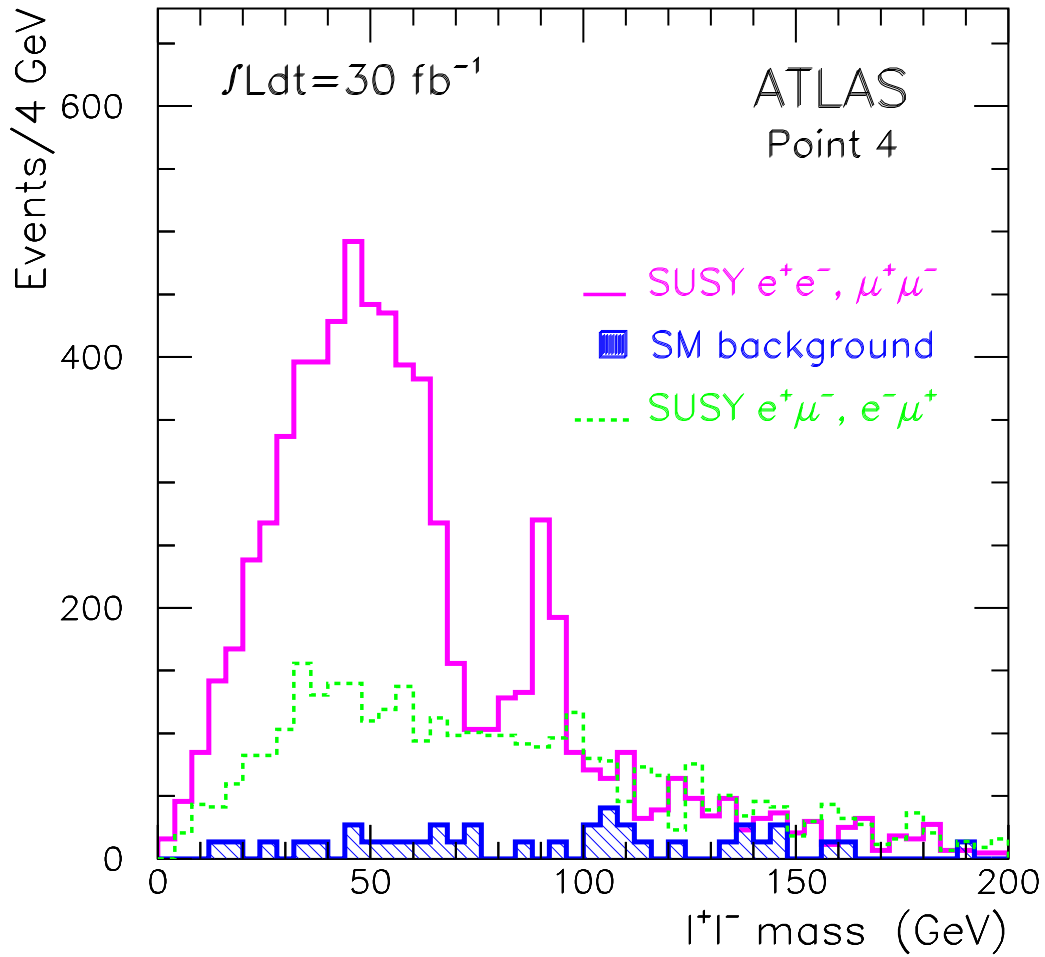


Figure 10: *Expected di-lepton invariant mass distributions for SUSY events containing opposite-sign opposite-flavour lepton pairs (dashed histogram), opposite-sign same-flavour pairs (full histogram), and for $t\bar{t}$ events containing opposite-sign same-flavour pairs (dashed histogram), for an integrated luminosity of $3 \cdot 10^4 \text{ pb}^{-1}$.*

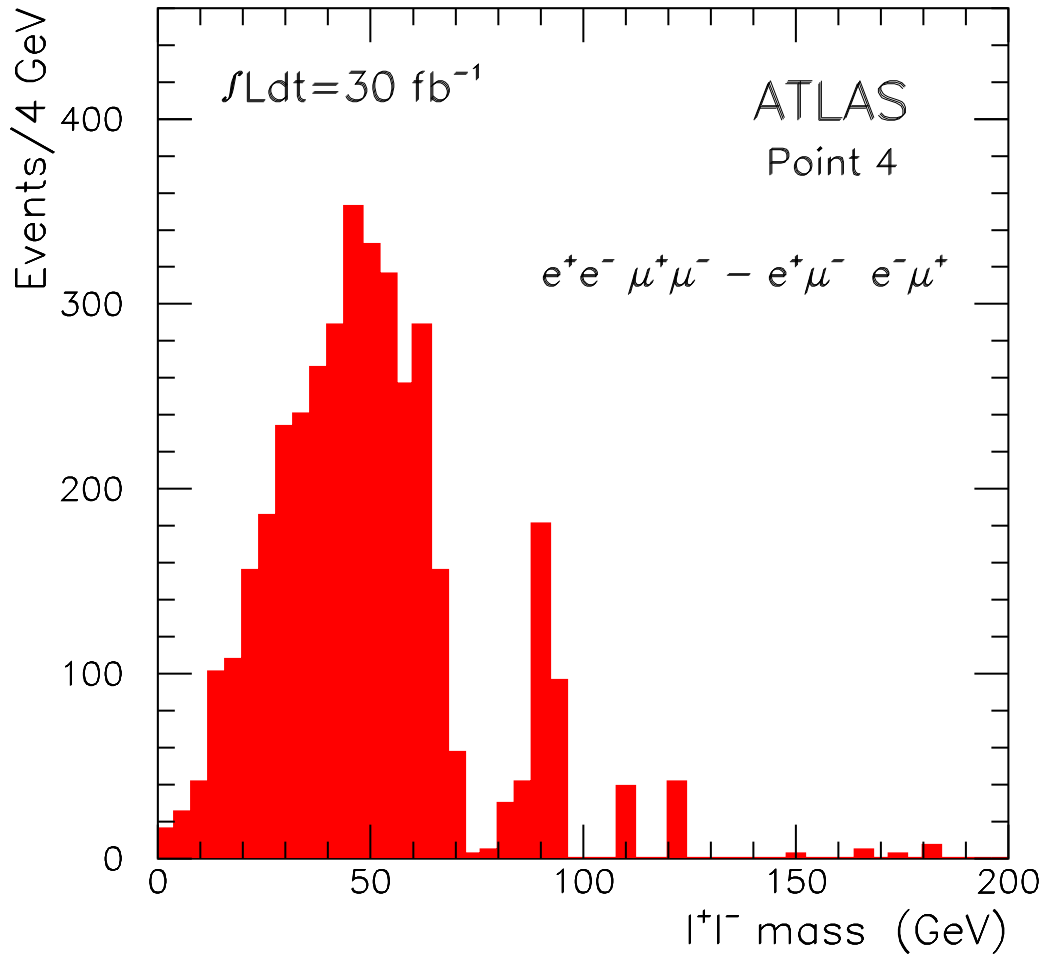


Figure 11: *Expected di-lepton invariant mass distribution for events containing OS-SF lepton pairs (SUSY plus background), after subtraction of events containing OS-OF lepton pairs, for an integrated luminosity of $3 \cdot 10^4 \text{ pb}^{-1}$.*

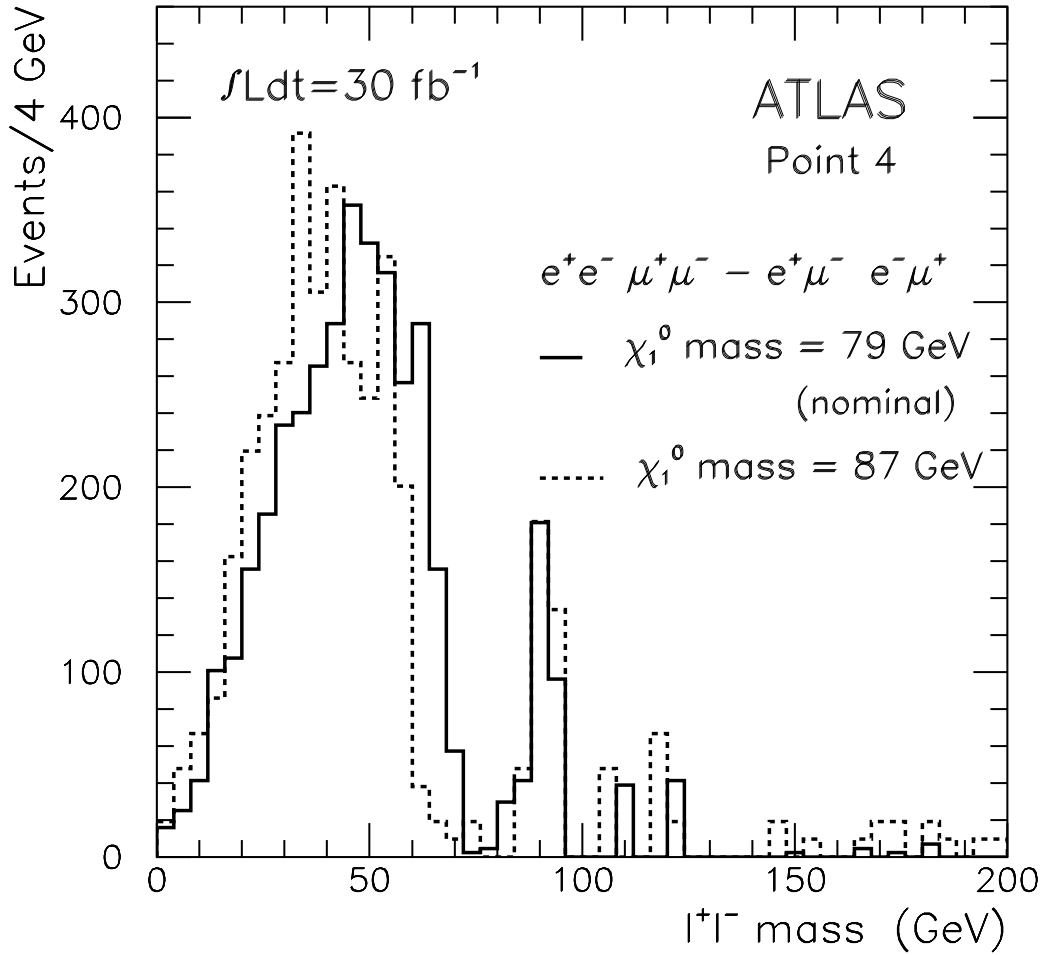


Figure 12: *Expected di-lepton invariant mass distributions for events containing OS-SF lepton pairs (SUSY plus background), after subtraction of events containing OS-OF lepton pairs, for an integrated luminosity of $3 \cdot 10^4 \text{ pb}^{-1}$ and for two values of the χ_1^0 mass: $m_{\chi_1^0} = 79 \text{ GeV}$ (full histogram) and $m_{\chi_1^0} = 87 \text{ GeV}$ (dashed histogram).*

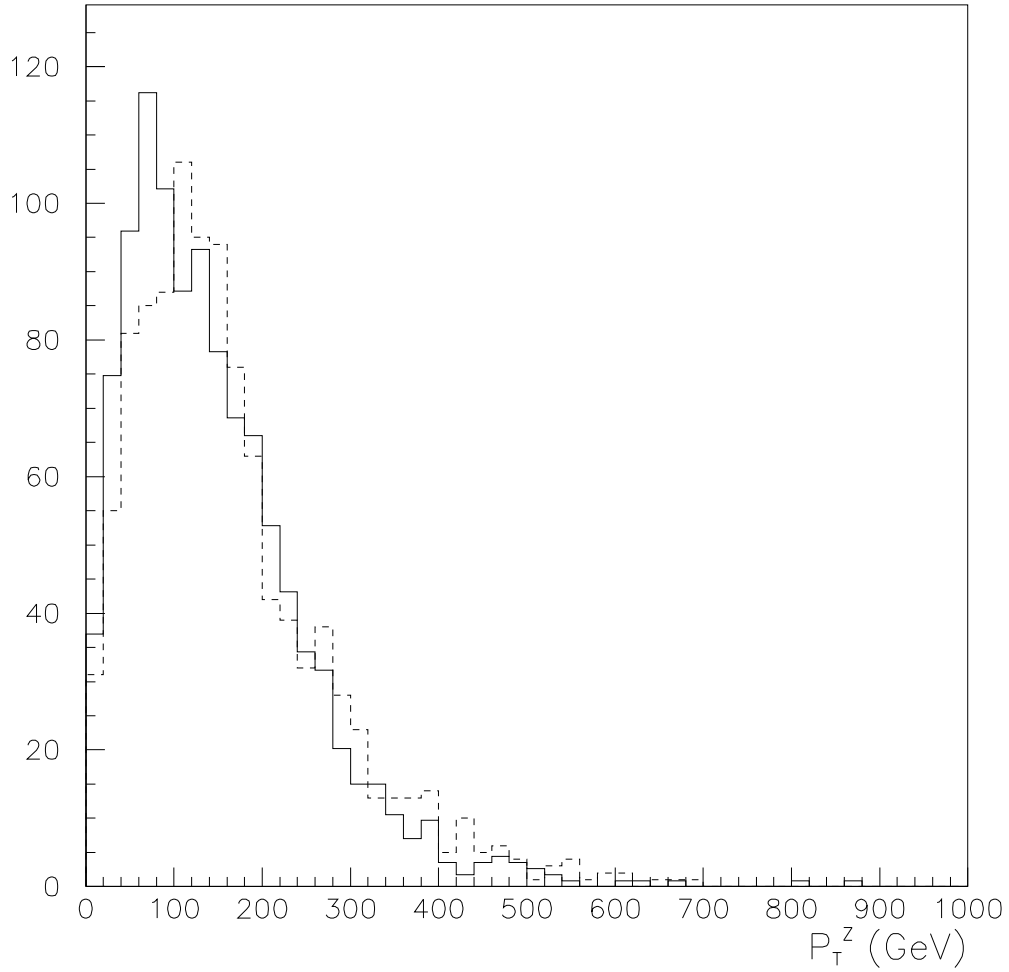


Figure 13: *Distributions of the reconstructed transverse momentum of the Z bosons produced in χ_2^\pm decays at Point 4 for $m_{\chi_2^\pm} = 315$ GeV (solid histogram) and $m_{\chi_2^\pm} = 360$ GeV (dashed histogram).*

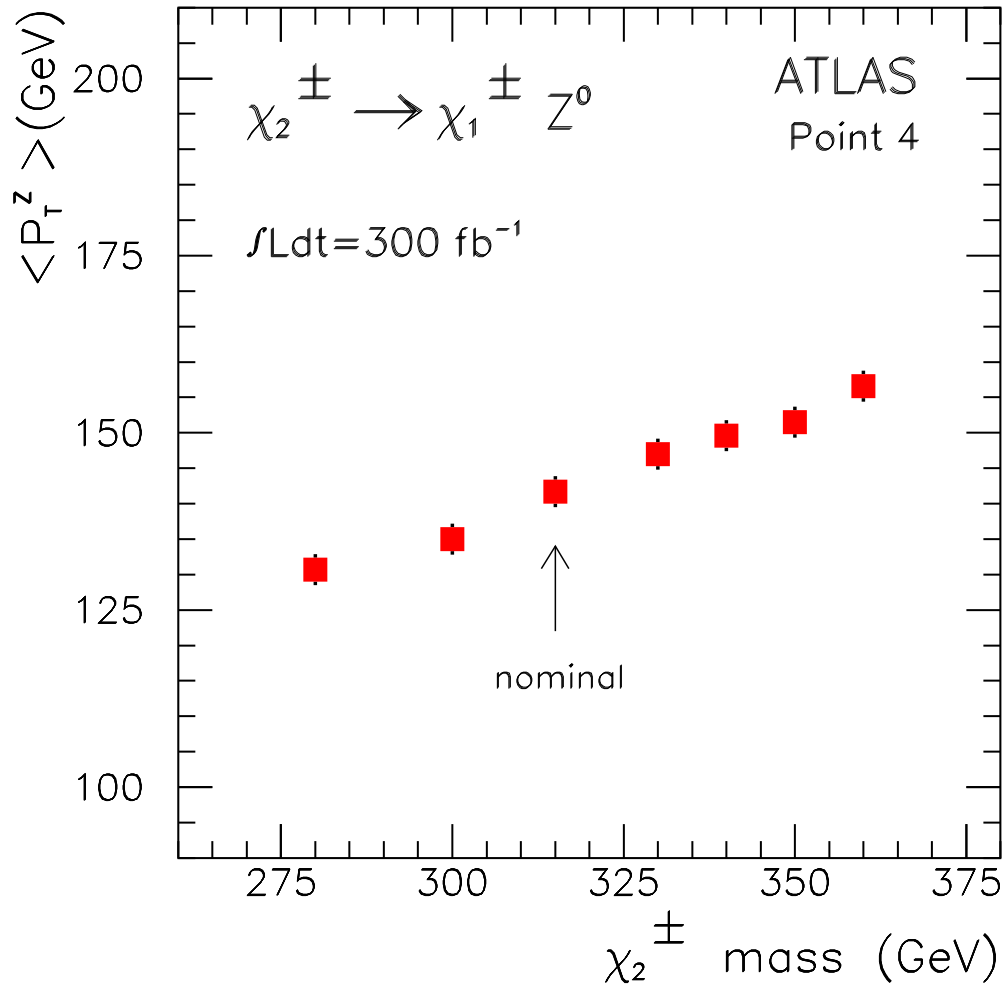


Figure 14: Average value of the p_T distribution of the Z bosons produced in χ_2^\pm decays at Point 4, as a function of the χ_2^\pm mass. The error bars correspond to the summed statistical and systematic error for an integrated luminosity of $3 \cdot 10^5 \text{ pb}^{-1}$.

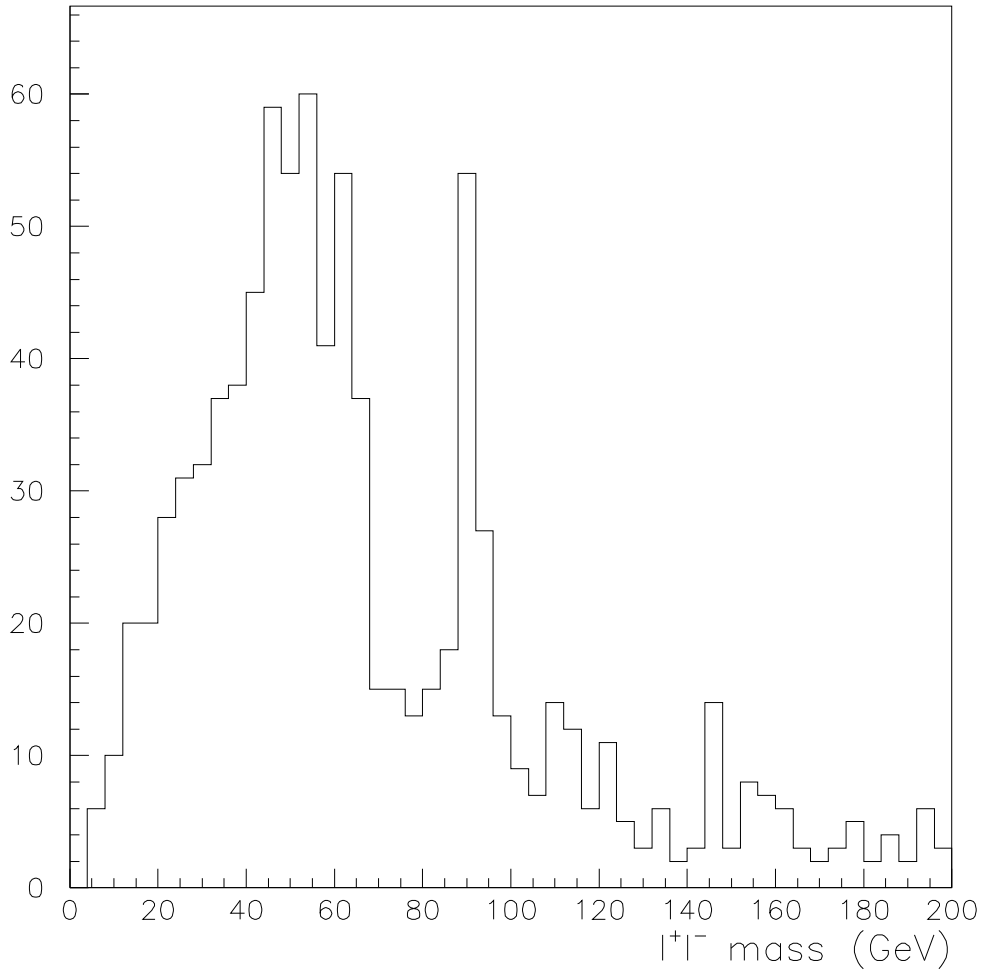


Figure 15: *Di-lepton invariant mass distribution for SUSY events at Point 4 containing three leptons and four jets in the final state.*

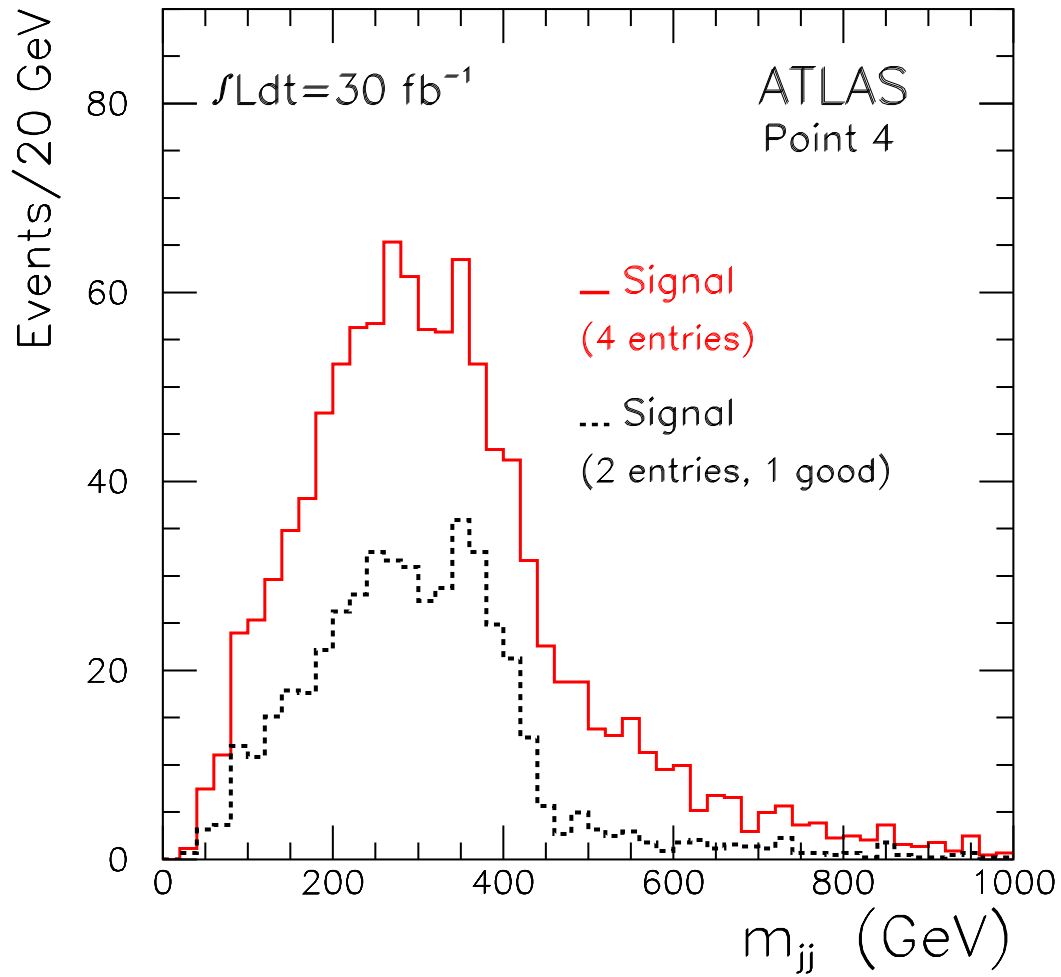


Figure 16: *Expected di-jet invariant mass distribution for SUSY events with two gluinos in the final state (full histogram). Four jet pairs are plotted per event (see text). The dashed histogram shows the distribution obtained when only the combination with at least one correct jet pair is considered (see text).*

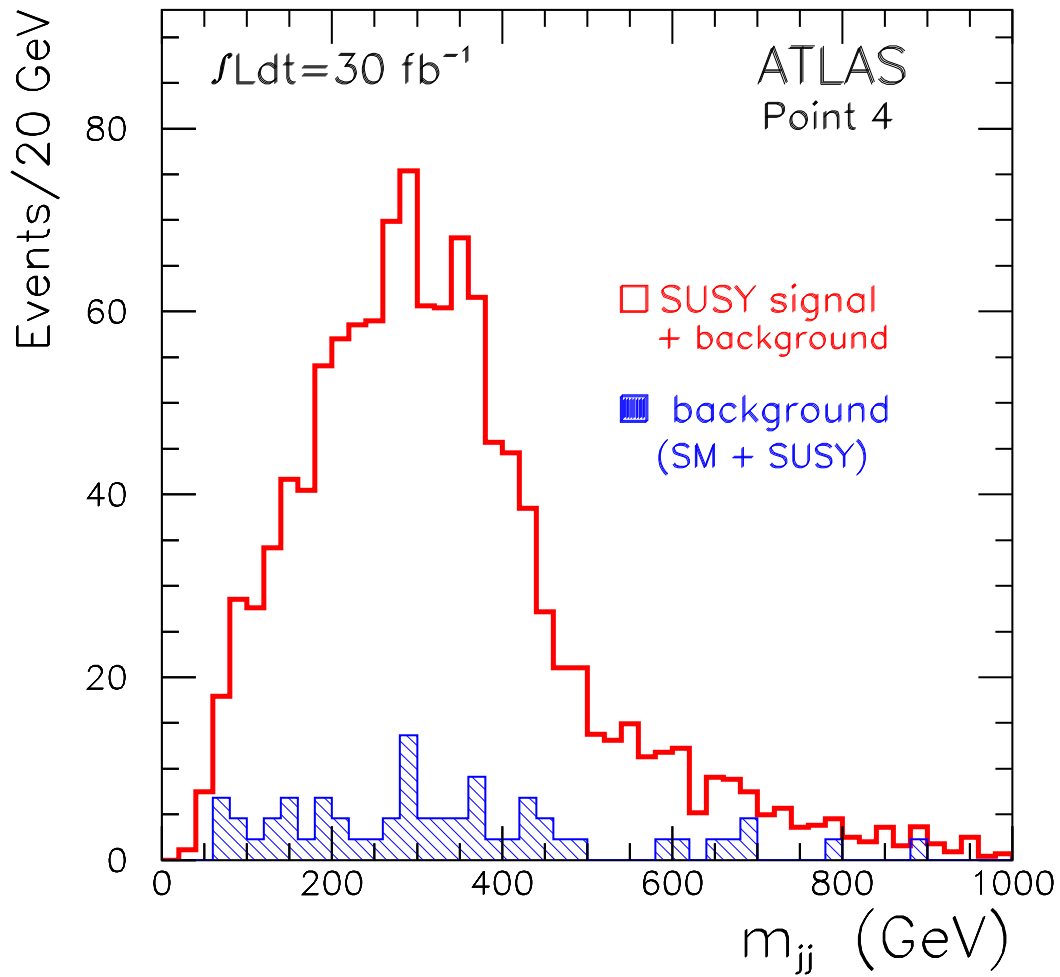


Figure 17: *Di-jet invariant mass distributions for events with three leptons and four jets in the final state. The full histogram is the expected distribution for the SUSY signal plus background and the dashed histogram for the background alone, for an integrated luminosity of $3 \cdot 10^4 \text{ pb}^{-1}$. Four jet pairs are plotted per event (see text).*

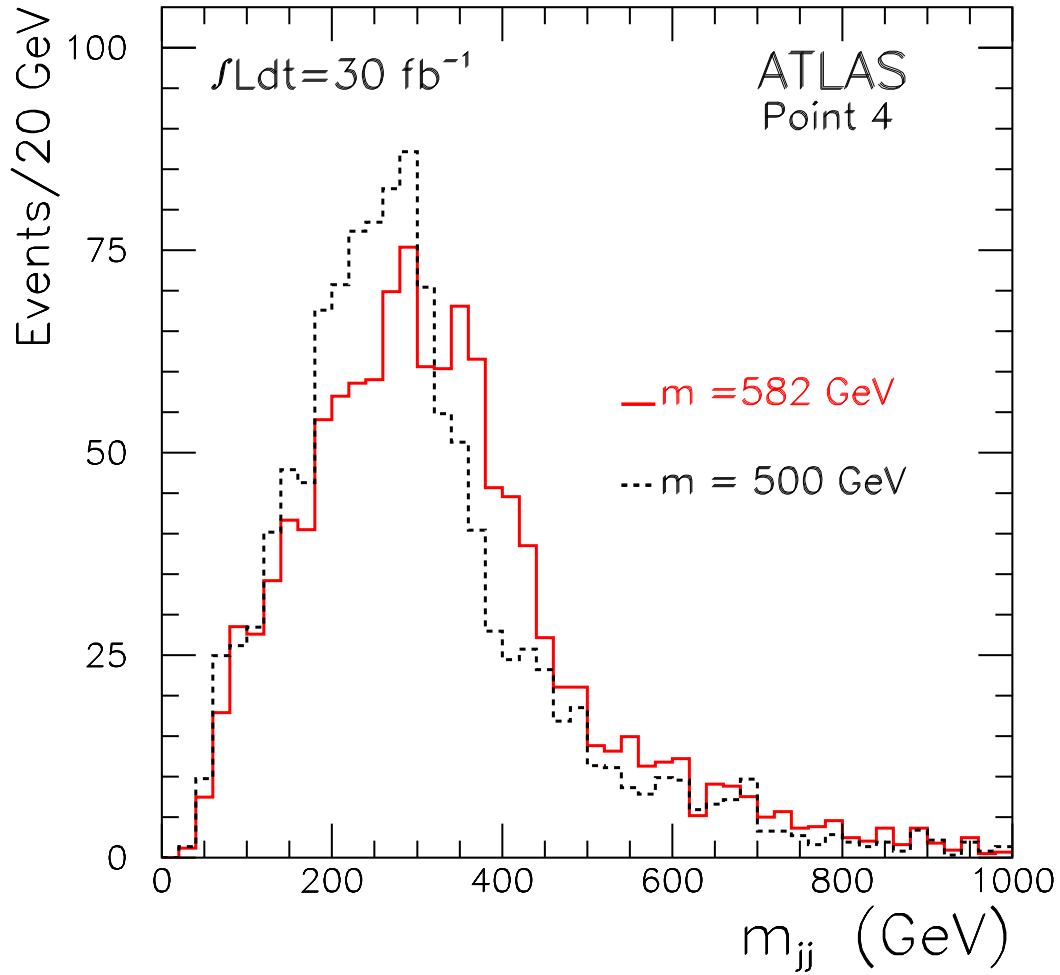


Figure 18: *Di-jet invariant mass distributions for events with three leptons and four jets in the final state. The sum of the expected SUSY signal and backgrounds ($t\bar{t}$ and SUSY combinatorics) is shown for an integrated luminosity of $3 \cdot 10^4 \text{ pb}^{-1}$. The solid histogram is for $m_{\tilde{g}} = 582 \text{ GeV}$ and the dashed histogram for $m_{\tilde{g}} = 500 \text{ GeV}$. Four jet pairs are plotted per event (see text).*

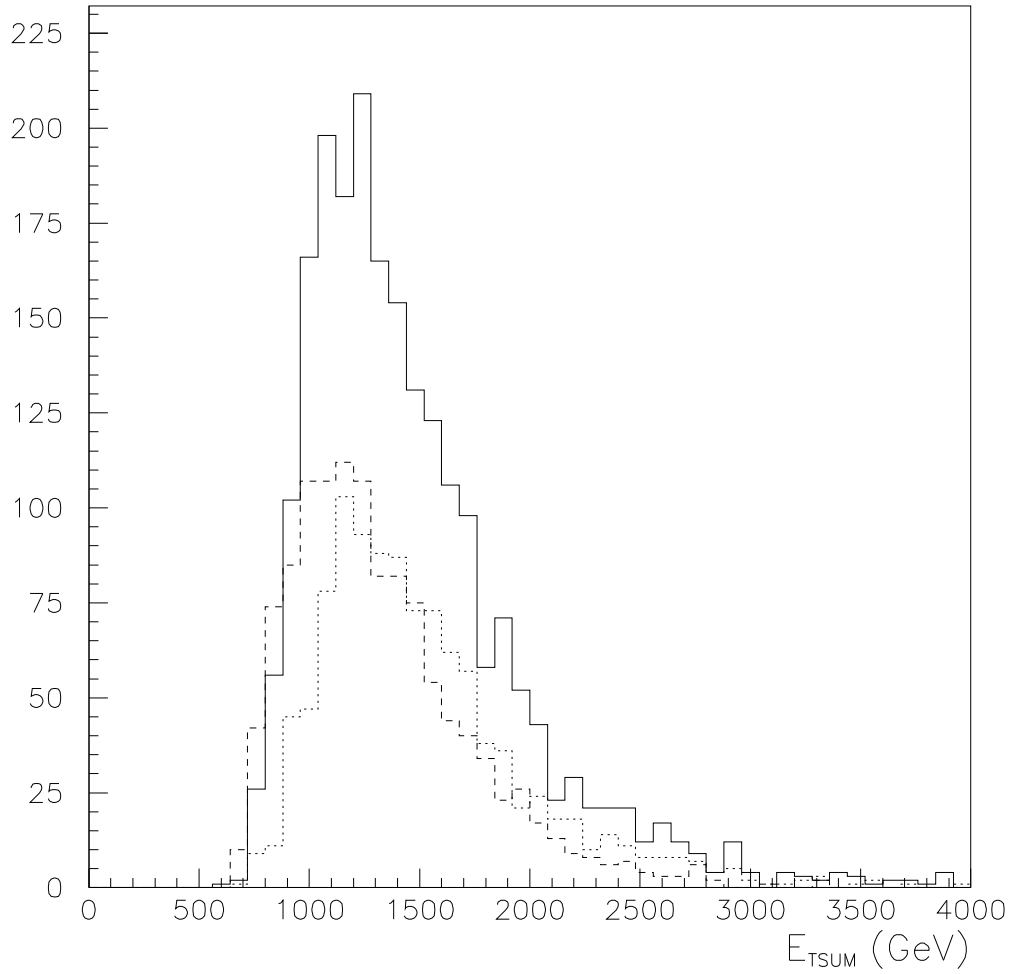


Figure 19: *Distribution of the variable E_{Tsum} (see text) for SUSY events from $\tilde{g}\tilde{q}$ production (solid histogram), $\tilde{g}\tilde{g}$ production (dashed histogram) and $\tilde{q}\tilde{q}$ production (dotted histogram).*

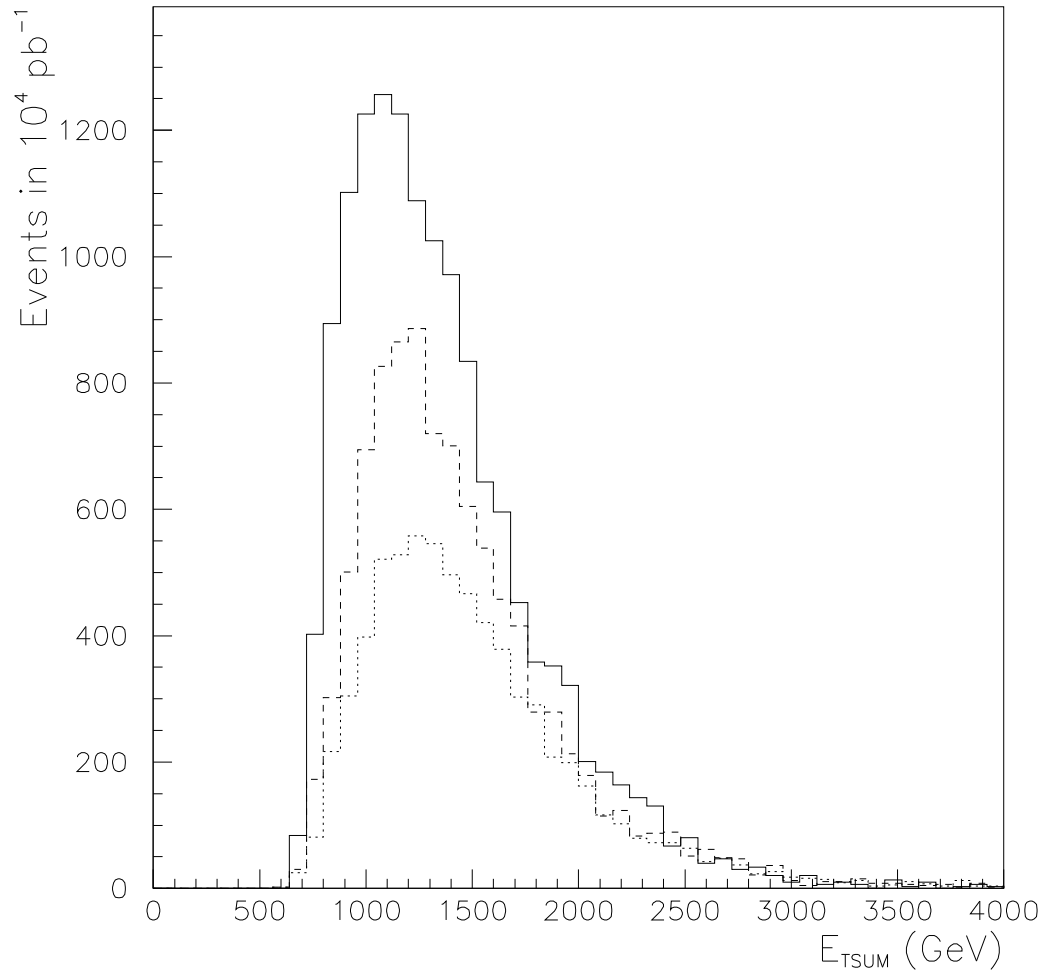


Figure 20: *Distribution of the variable $E_{T\text{sum}}$ for selected samples of SUSY events at Point 4 (see text) with $\langle m_{\tilde{q}} \rangle \simeq 715 \text{ GeV}$ (solid histogram), $\langle m_{\tilde{q}} \rangle \simeq 915 \text{ GeV}$ (dashed histogram) and $\langle m_{\tilde{q}} \rangle \simeq 1115 \text{ GeV}$ (dotted histogram).*

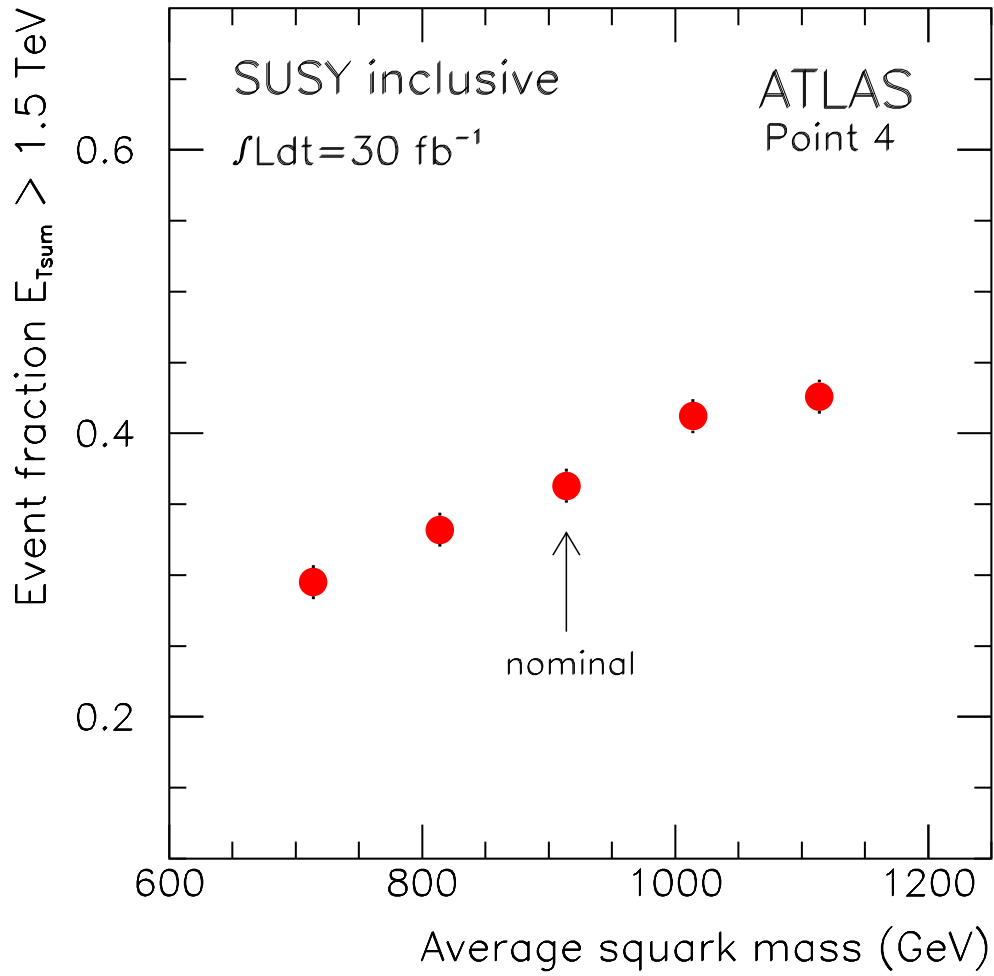


Figure 21: *Fraction of selected SUSY events with $E_{Tsum} > 1500 \text{ GeV}$ as a function of the average squark mass. The error bars correspond to the summed statistical and systematic error for an integrated luminosity of $3 \cdot 10^4 \text{ pb}^{-1}$.*

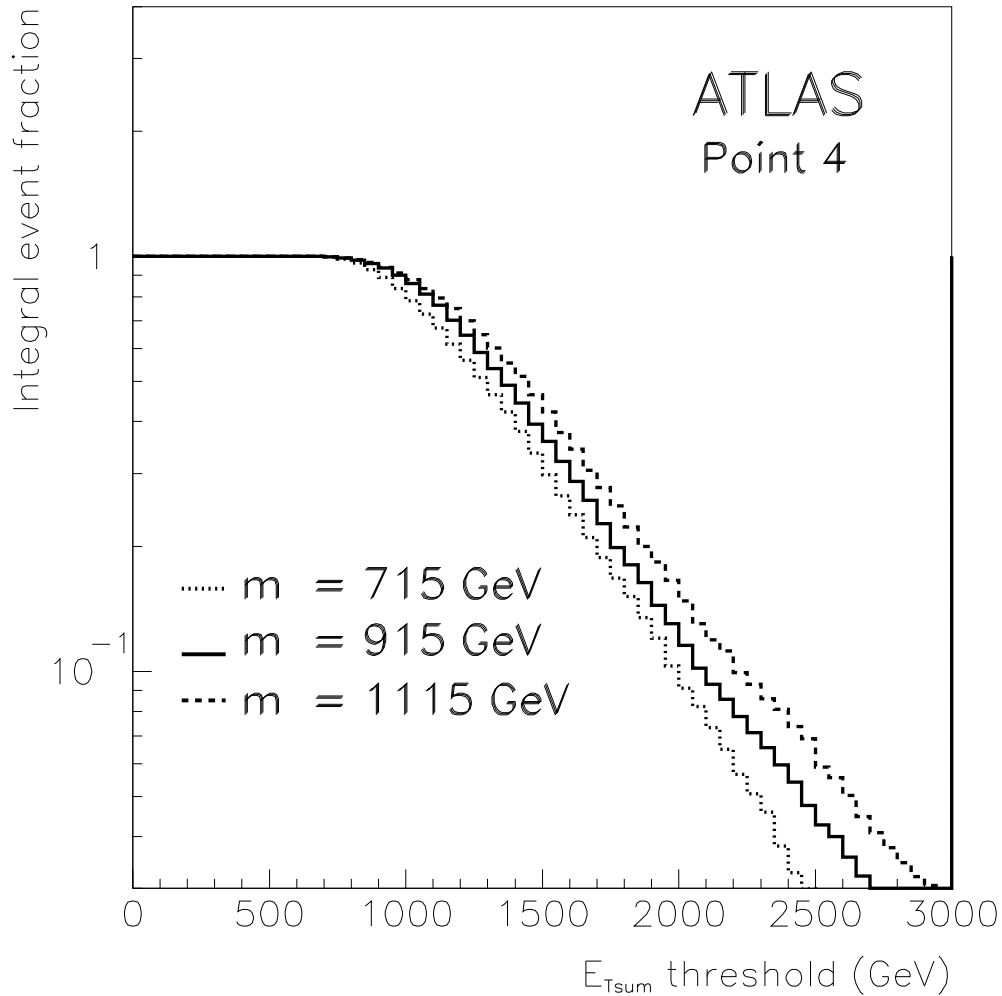


Figure 22: Fraction of selected SUSY events at Point 4 with E_{Tsum} larger than a given threshold for $\langle m_{\tilde{q}} \rangle \simeq 715 \text{ GeV}$ (dotted histogram), $\langle m_{\tilde{q}} \rangle \simeq 915 \text{ GeV}$ (full histogram) and $\langle m_{\tilde{q}} \rangle \simeq 1115 \text{ GeV}$ (dashed histogram).